frontiers in Earth Science

ORIGINAL RESEARCH
published: 08 March 2022
doi: 10.3389/feart.2022.846997

Magma and Mineral Composition Response to Increasing Slab-Derived Fluid Flux: Nevado de Longaví Volcano, Southern Chilean Andes

Daniel Sellés[1,2]*, *Michael Dungan*[3], *Charles Langmuir*[1], *Ana Carolina Rodríguez*[1,4] and *William P. Leeman*[5]

[1]Department of Earth and Planetary Sciences, Harvard University, Cambridge, MA, United States, [2]Teck Resources Chile Ltda, Santiago, Chile, [3]Courtesy Professor Department of Earth Sciences, University of Oregon, Eugene, OR, United States, [4]Corporación Nacional Del Cobre CODELCO, Santiago, Chile, [5]Department of Earth, Planetary and Environmental Sciences, Rice University, Houston, TX, United States

Nevado de Longaví volcano (NLV), in the Southern-Central Chilean Andes, has erupted during the Holocene magmas with compositions that are in several ways atypical for the region. These characteristics include elevated La/Yb ratios in evolved magmas, in an area of only moderately thick crust, coupled with low concentrations of K, Th, and other incompatible elements and elevated ratios of fluid-mobile (B, Cs, Li, Sb) to fluid-immobile elements. Samples have an unusual mafic mineralogy dominated by amphibole. The petrology of the Holocene products of NLV have been related to the influence of an oceanic transform fault (Mocha Fracture Zone; MFZ) that supplies the mantle wedge with unusually high amounts of fluids via dehydration of serpentinite bodies hosted by the subducted oceanic lithosphere. Because the trace of this transform fault is oblique to the convergence vector, its position along the arc has varied through time, as has the magnitude of its influence on the nature of the magmas erupted at NLV. The whole-rock and mineral chemistry of volcanic products from NLV, tied to a simplified stratigraphy, documents the secular changes in the magmatic system as the oceanic fault approached its current position. Magmas erupted ~1–0.6 Ma are relatively low in water (as inferred from mineralogy and chemical proxies) and reduced (NNO-1 to NNO+0.5), and are similar to compositions found in neighboring volcanoes. From 0.25 Ma to the present, magmas are water-rich and oxidized (NNO-0.5 to NNO+1.7). In the intervening 0.6–0.25 Ma, mafic magmatism acquired a transient crustal component, which we identify as subducted sediment melts, on the basis of radiogenic isotopes and Pb, Th, and U abundances. Fluids released from serpentinite in the fracture zone were rich in Li, B, Sb, Cs and Ba, but not in K, Th, U and Sr. The fluid addition led to enhanced melting, particularly hydrous magmas that stabilized amphibole early during fractionation, higher oxygen fugacities, and distinctive chemical compositions.

Keywords: Oceanic fracture zone, Serpentinite, Adakite, Hydrous magmas, Andes, Southern Volcanic Zone, Amphibole

OPEN ACCESS

Edited by:
Scott Andrew Whattam, King Fahd University of Petroleum and Minerals, Saudi Arabia

Reviewed by:
Susanne Martina Straub, Columbia University, United States
Takeshi Kuritani, Hokkaido University, Japan

***Correspondence:**
Daniel Sellés
dselles@gmail.com

Specialty section:
This article was submitted to Petrology, a section of the journal Frontiers in Earth Science

Received: *31 December 2021*
Accepted: *15 February 2022*
Published: *08 March 2022*

Citation:
Sellés D, Dungan M, Langmuir C, Rodríguez AC and Leeman WP (2022) Magma and Mineral Composition Response to Increasing Slab-Derived Fluid Flux: Nevado de Longaví Volcano, Southern Chilean Andes. Front. Earth Sci. 10:846997. doi: 10.3389/feart.2022.846997

1 INTRODUCTION

Subduction-related magmatism involves multiple geological reservoirs, which successively add elemental and isotopic contributions to the diverse geochemical signatures of magmas that reach the Earth's surface. Subducted oceanic lithosphere, composed of altered oceanic crust, variably hydrated mantle, and sediments, releases water-rich fluids during prograde metamorphic reactions and may partially melt with increasing pressure and temperature. The upward migration of these water-rich phases leads to metasomatic modifications of the asthenospheric mantle wedge, and in sufficient quantities may trigger partial melting of mantle peridotite. Primitive magmas that include mantle- and slab-derived contributions are subsequently further modified as they ascend, crystallize, and interact with lithologies in the overriding plate. Individual components or processes may be identifiable on the basis of distinctive isotopic or elemental features in the erupted magmas, but our ability to resolve the details of magma genesis is hampered by limited knowledge of the compositions of deep reservoirs.

One potential water reservoir is serpentinite formed by hydration of oceanic mantle lithosphere, through permeability pathways in the crust such as fracture zones and normal faults developed during bending of the plate at the trench (Ranero et al., 2003; Moscoso and Contreras-Reyes, 2012; Manea et al., 2014). The influence of fracture zone subduction on the nature of magma composition has not been thoroughly studied. Grove et al. (2002) suggested that serpentinites hosted in the Blanco fracture zone subducting beneath Mt. Shasta volcano in the Cascades arc might account for the isotopic character of the highly hydrous lavas. For the Aleutian arc, Singer et al. (1996), Jicha et al. (2004), and Singer et al. (2007) documented the trace element and isotopic characteristics of Seguam volcano, which is located above the Amlia fracture zone. In the Mexican volcanic belt, Manea and Manea (2008) have shown that the geophysical signature of a serpentinized fracture zone (the Tehuantepec FZ) can be traced beneath the continental plate and to project beneath El Chichón volcano, another strange adakitic center. Whalen et al. (2003) speculated that the Th-depleted signature of a ~3 Ga arc-related intrusive complex was a consequence of a localized source of serpentine-derived fluids, probably related to a subducting fracture zone.

In this contribution we examine the case of Nevado de Longaví volcano (NLV) in the Southern Volcanic Zone of the Andes (SVZ), which is currently located above the projection of the oceanic Mocha Fracture Zone (MFZ). We examine the changing local magma generation conditions as the MFZ approaches its current position in the framework of a simplified stratigraphy supported by geochronology.

2 GEODYNAMIC SETTING AND SVZ MAGMATISM

The Southern Volcanic Zone (SVZ) of the Andes has developed on the active western margin of the South American plate between the latitudes where the aseismic Juan Fernandez Ridge (33°S) and the actively spreading Chile Rise (46.5°S) are being subducted (**Figure 1A**). Summit elevations of SVZ frontal arc volcanoes decrease steeply from nearly 6,000 m asl at the northern end (~33.4°S) to ~3,500 m asl at 36°S, and elevations decrease to the south of this latitude to only slightly less than 3,000 m at 41°S (**Figure 1B**). The thickness of the crust underlying the northernmost SVZ centers also decreases from ~60 to ~40 km between 33°S and 36°S, due partly to the fact that the northern part of the volcanic front trends obliquely with respect to the Andean axis. Volcanoes at 33–34°S are located on the Andean crest, whereas by 36-37°S the volcanic front is ~50 km to the west of the continental divide, and to the south of this latitude the volcanic front trends parallel to the cordilleran axis. Crustal thickness beneath the volcanoes decreases less steeply to ~30 km at 41°S (Hildreth and Moorbath, 1988; Tassara et al., 2006; Tasárová, 2007). The proportion of felsic upper crust also decreases from north to south as indicated by elastic thickness and flexural analysis, which suggest that the rheology of the crust is quartz-dominated in the north, whereas to the south the crust is stiffer, more dominated by plagioclase-rich lithologies (Tassara and Yañez, 2003; Tassara et al., 2006).

Systematic variations in the compositions of magmas along the SVZ can be related to changes in the nature of the underlying crust. Volcanoes in the northern part of the SVZ have elevated crustal contributions that have been explained either as the result of lower crustal assimilation (Hildreth and Moorbath, 1988; **Figure 1C**) or as mantle-source contamination by forearc tectonic erosion (Stern, 1991; Kay et al., 2005). Along-strike variations in the mean extent of mantle melting and average depth of differentiation have also been invoked to account for some of the trace element characteristics of arc magmas along the arc (Tormey et al., 1991), and have more recently been shown to exert the main control on primitive magma variation along the Andean SVZ (Turner et al., 2016; Turner et al., 2017).

Arc magmas are generally less evolved and have generally lower crustal imprint south of 36°S due to both the more refractory nature of the crust and magma ascent facilitated by lithosphere-scale faults. The ~1,000 km long strike-slip Liquiñe-Ofqui fault zone parallels the arc and controls the emplacement of some volcanoes south of 37°S, where it terminates in the retroarc region (López-Escobar et al., 1995a; Folguera et al., 2004).

Nevado de Longaví volcano (hereafter NLV; 36.2°S) is at an inflection point in terms of regional magmatic and geodynamic gradients. This is due in part to the projection of the oceanic Mocha Fracture Zone (MFZ) in the Nazca plate beneath the arc at this latitude (dip-corrected for 30° subduction angle; Bohm et al., 2002). The MFZ trends obliquely (N60°) to other fracture zones of the Nazca plate (N80°; Valdivia and Chiloé F.Z. in **Figure 1**), and it is the locus of a ~5 My age offset in subducting plate age at the trench (Tebbens et al., 1997). The MFZ and the Challenger FZ further north displace crust generated by the Pacific-Farallon spreading center (East Pacific Rise), whereas the fractures to the south were generated at the Antarctic-Nazca spreading center (Chile Ridge; Herron, 1981; Tebbens and Cande, 1997). The MFZ is also oblique to the current convergence vector (~N78E, ~8 cm/y; NUVEL-1A model), and thus its intersection with the arc front migrates southwards at a rate of ~20 km/My.

The presence of the Mocha Fracture Zone beneath NLV has been related to some of the chemical and mineral characteristics of Holocene NLV lavas (Sellés et al., 2004; Rodríguez, 2006; Sellés, 2006; Rodríguez et al., 2007). Serpentinization of the oceanic mantle by circulation of seawater through permeability pathways

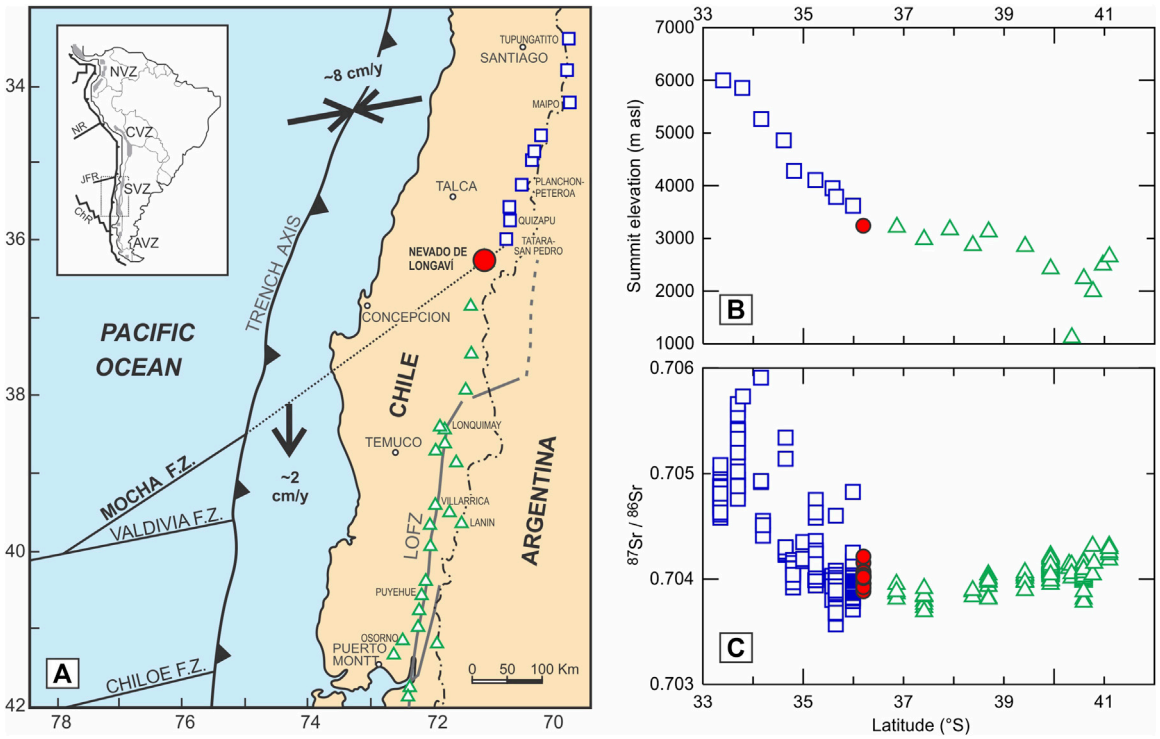

FIGURE 1 | (A) Location of Nevado de Longaví volcano in the Andean Southern Volcanic Zone and dip-corrected projection of the Mocha Fracture Zone. NVZ, CVZ, SVZ, and AVZ in inset stand for the Northern, Central, Southern, and Austral Volcanic Zones. NR, JFR and ChR correspond to the Nazca Ridge, Juan Fernandez Ridge, and Chile Rise, respectively. **(B)** Along-arc variation in summit elevation of arc-front volcanoes of the SVZ. **(C)** $^{87}Sr/^{86}Sr$ ratios along the SVZ. (Data from Harmon et al., 1984; López-Escobar et al., 1985; Hickey et al., 1986; Futa and Stern, 1988; Gerlach et al., 1988; Hildreth and Moorbath, 1988; Hickey-Vargas et al., 1989; McMillan et al., 1989; Tormey et al., 1991; López-Escobar et al., 1992; Hilton et al., 1993; Tagiri et al., 1993; López-Escobar et al., 1995a; Tormey et al., 1995; Feeley et al., 1998; Déruelle and López-Escobar, 1999; Costa and Singer, 2002; Jicha et al., 2007).

in the oceanic crust has been observed elsewhere, including oceanic fracture zones such as the MFZ (Peacock, 2001; Hyndman and Peacock, 2003; Whalen et al., 2003; Manea and Manea, 2008). Dehydration of serpentinite bodies hosted in the subducted part of the MFZ has been proposed as a mechanism to flux the asthenospheric mantle with unusually high amounts of fluids to produce wet, high-degree melts from which Holocene NLV dacites are derived (Rodríguez et al., 2007). As the subducted Mocha Fracture Zone is not stationary with respect to the continental margin, its impact on magmatism is also expected to change through time. We document temporal changes in chemical and petrologic characteristics through a sequence of Early Pleistocene to Holocene lavas. Whole-rock and mineral chemistry data are presented in a revised stratigraphic framework calibrated by $^{40}Ar/^{39}Ar$ ages. We identify and quantify different reservoirs involved in magma generation as the MFZ approached its current location beneath NLV and conclude that the variations in the magmatic signatures through time are consistent with increasing magmatic water contents.

3 VOLCANIC STRATIGRAPHY

Early Pleistocene-Quaternary volcanoes in the NLV area are constructed on volcaniclastic strata of late Oligocene-early Miocene age and middle to late Miocene granitoids. The 2–3 km thick volcaniclastic sequence, known in this area as the Cura-Mallín Formation is composed mainly of andesitic tuffs and breccias, plus subordinate lava flows and continental sedimentary strata of fluvial and lacustrine facies with low-degree burial metamorphism (Muñoz and Niemeyer, 1984; Jordan et al., 2001). These units were deposited in intra-arc extensional basins, and the associated volcanic rocks are isotopically primitive tholeiites with insignificant crustal contamination (Vergara et al., 1999). The Cura-Mallín Formation was folded during Miocene basin inversion and crustal shortening. Batholith-scale granitoid plutons of middle Miocene age intruded to the west of the Quaternary arc, and small late Miocene stocks and plutons crop out in the vicinity of active volcanoes (Muñoz and Niemeyer, 1984). These are biotite and amphibole-bearing quartz-diorites to tonalites plus granodiorites.

3.1 Pre-Longaví Volcanic Rocks (Early Pleistocene)

Unit 0: Early Pleistocene volcanism between 36 and 37°S (whole-rock K-Ar ages of 1.7 ± 0.7, 1.35 ± 0.13, 0.9 ± 0.5 Ma) is regionally mapped as the Cola de Zorro Formation (Muñoz and Niemeyer, 1984). This formation is represented near NLV by a deeply dissected, mainly mafic stratocone complex named Villalobos volcano. The inferred

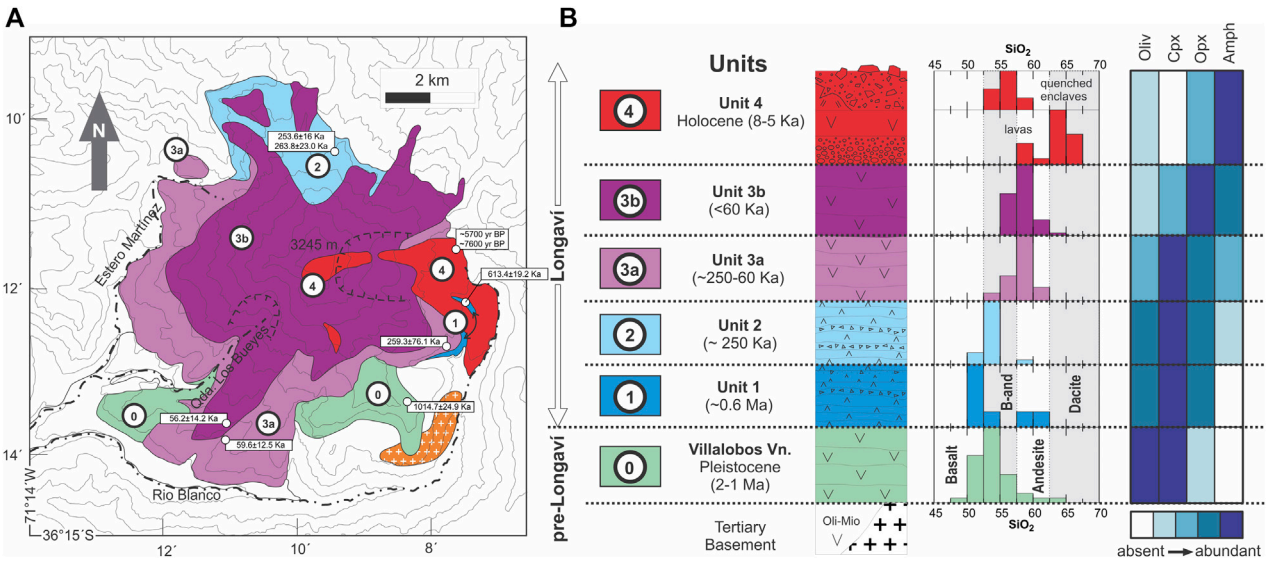

FIGURE 2 | (A) Geological sketch of Nevado de Longaví volcano showing the distribution of units discussed in the text (topographic contours every 200 m) and approximate location of dated samples. Right: Schematic stratigraphic column and silica-frequency histograms for analyzed samples from each unit, showing a tendency towards increasingly evolved magmas being erupted with time. Relative ferromagnesian phase abundances **(B)** also show a tendency of increasing amphibole involvement at the expense of pyroxenes. Note that relative mineral abundance is valid for Unit 4 mafic enclaves and lavas.

vent is located ~10–15 km south of the NLV summit, but the northernmost flank remnants are uncomformably overlain by younger lavas from the NLV edifice (**Figure 2**). A $^{40}Ar/^{39}Ar$ age on groundmass of a lava flow underlying NLV lavas on the SW flank of NLV is 1,015 ± 25 Ka (**Supplementary Material S1**). Unit 0 lavas are mainly basalts and basaltic andesites (50–55 wt% SiO_2), although andesites and more evolved compositions are also present in lower proportions.

3.2 Internal Stratigraphy of Nevado de Longaví Volcano

Nevado de Longaví volcano is a comparatively small, single cone (summit altitude 3,242 m–9 km diameter, ~20 km^3 estimated volume), mainly composed of thick andesitic flows that radiate from the current summit area. There are no large pyroclastic deposits suggestive of caldera-forming eruptions during the history of the volcano, but sector collapse scars are present on the eastern and southwestern slopes of the cone (**Figure 2**). Deep incisions into the northern and eastern flanks of the volcano expose relatively old sequences of lavas referred to as the Basal Units.

3.2.1 Basal Longaví Units (Units 1 and 2)

Unit 1: Basal unit of the eastern flank: The eastern flank of the volcano appears to have undergone a pre-Holocene structural collapse that created a large topographic bowl which is currently filled by Holocene pyroclastic deposits. A ~50 m thick sequence consisting mainly of mafic lavas, breccias, and intercalated coarse- and fine-grained volcano-sedimentary deposits is exposed around the southern margin of the collapse scar and in some of the canyons excavated through younger deposits. This sequence is largely buried by Holocene deposits and main cone lavas (dated at ~260 Ka; see below) immediately south of the collapse depression. A total fusion age of 613 ± 19 Ka (no plateau) was obtained from a basaltic lava flow within this sequence.

All lava samples from this unit are basaltic andesites (52–53 wt % SiO_2) with abundant plagioclase, olivine and clinopyroxene, plus lesser orthopyroxene phenocrysts and microphenocrysts. Vitrophyric, prismatically jointed blocks (~20 cm) of more evolved compositions (55–62 wt% SiO_2) were also collected from volcaniclastic breccias. These andesitic fragments contain the same mineral phases as the basalts, but orthopyroxene is more abundant than olivine and clinopyroxene.

Unit 2: Basal unit of the northern flank: This sequence is exposed in deep glacial incisions on the north flank of the volcano. This unit formed a ~600–700 m high cone with its vent located ~1,500 m to the north of the current summit that was later almost completely covered by thick Main Cone lavas. The most deeply exposed part of this unit consists of a few thick (>6 m) andesitic to basaltic andesitic flows (53.8–58.4 wt% SiO_2) that are overlain by more numerous but thin (1–3 m) basaltic andesitic flows (52–55 wt% SiO_2). One andesitic lava flow from the deep section and one overlying basaltic andesitic flow yielded $^{40}Ar/^{39}Ar$ plateau ages of 264 ± 23 ka and 254 ± 16 Ka respectively (**Supplementary Material S1**).

3.2.2 Main Cone Andesites (Units 3a and 3b)

The bulk of the edifice consists of thick andesitic flows (55–63% SiO_2) that radiate from a vent area coincident with the current topographic summit. Main cone lavas exhibit greater chemical and mineralogical diversity than other units of the volcano, and they are texturally more complex. A useful distinction among main cone lavas is the degree of enrichment in incompatible elements as silica increases. Two divergent differentiation trends

in terms of Rb and other incompatible element enrichments are referred to as High-Rb and Low-Rb series (Sellés et al., 2004). This distinction among Main Cone lavas is based on chemical criteria rather than a clear stratigraphic superposition. There is a marked tendency for old lavas in several sections around the volcano to be relatively Rb-enriched. Less enriched lavas, which tend to be stratigraphically higher, generally have higher modal proportions of amphibole. This mineralogical tendency is not sufficiently marked to permit rigorous macroscopic identification of these two compositional series, as modal mineralogy also varies with degree of evolution. Nor are there unambiguous chemical distinctions for some andesitic samples that are chemically intermediate between the most extreme examples of these two trends. Despite the lack of binary mineralogical and chemical shifts from early to late main-cone andesites, these lavas record a progression from early magmatism with dominantly anhydrous minerals to the Holocene amphibole-rich magmas (**Figure 2**).

Unit 3a: This unit is composed of LILE-enriched andesites with 56–62 wt% SiO_2 (which range down to 54 wt% SiO_2 when quenched mafic enclaves are considered). An andesite near the east base, overlying clastic beds assigned to Unit 1, yields a plateau age of 259 ± 76 Ka. A second sample from the south flank, underlying relatively low-Rb flows, was dated at 60 ± 13 Ka. These flows form the lower portions of several sections around the volcano where they overlie Unit 2 lavas on the northern flank and Unit 1 on the east.

Unit 3b: Younger andesitic lava flows that form the outer shell of the Main Cone span a major element compositional range comparable to that of Unit 3a (56–62 wt% SiO_2), but with lower incompatible element contents. One sample from a section overlying Unit 3a lavas, yields a plateau age of 56 ± 14 Ka, thereby providing an indication that the transition to andesites with relatively low Rb occurred at ~60 Ka.

3.3.3 Holocene Eruptive Products

Most of the Holocene activity at NLV was concentrated in the summit area and within a preexisting collapse bowl on the eastern flank of the edifice. The Holocene sequence is composed of a dacitic pumice fall deposit (Río Blanco deposits of Rodríguez et al., 2007), followed by a thick andesitic lava (Castillo Andesite). The last eruptive event recorded at NLV consists of near-summit dome extrusion that in large part collapsed to the east forming block-and-ash flow deposits (Lomas Limpias deposits). The pumice fall and block-and-ash deposits were dated at ~7,600 years B.P. and ~5,700 years B.P. respectively (Rodríguez, 2006).

Unit 4: Both Holocene dacitic eruptions are similar in mineralogy and chemistry. The products of the early explosive eruption are slightly more evolved and glass-rich than the later dome-forming dacite (65.5 compared to 64–64.5 wt% SiO_2). The phenocryst mineralogy of the Rio Blanco and Lomas Limpias dacites is plagioclase, amphibole and orthopyroxene, with lesser Fe-Ti oxides, apatite, and sulfides; clinopyroxene is completely absent.

The Lomas Limpias dacite contains abundant quenched mafic enclaves with a broad range of compositions (53–59 wt% SiO_2). These have diktytaxitic textures (Bacon, 1986) with abundant acicular plagioclase and amphibole crystals. Some quenched mafic enclaves have sparse olivine phenocrysts, and rare plagioclase xenocrysts from the host dacite are present. Olivine phenocrysts are always mantled and partly replaced by Mg-hastingsitic amphibole with low TiO_2 (Rodríguez, 2006). Otherwise, quench-phases in the mafic enclaves are the same as those in the dacites and their mineral chemistry is similar. Residual glass pockets in the enclaves are rhyolitic in composition (~75 wt% SiO_2), as is the microcrystalline groundmass in the dacite.

A small andesitic lava-dome (60 wt% SiO_2) that erupted between the dacitic events has textural and chemical characteristics consistent with mixing of a resident dacitic magma and a mafic recharge component. This hybrid andesite contains minor quenched mafic enclaves that are similar to those in the dacitic lavas.

4 RESULTS: WHOLE-ROCK CHEMISTRY

4.1 Major Elements

Underlying Pleistocene volcanic rocks (Unit 0) are characterized by early Fe and Ti enrichments, and strong MgO, Al_2O_3, and CaO decreases from mafic to intermediate compositions, whereas K_2O and Na_2O contents increase sharply with increasing silica (**Figure 3**). These differentiation trends are typical of the arc tholeiite affinity displayed by Quaternary SVZ volcanoes south of NLV. The overlying Nevado de Longaví volcano is characterized by less steep decreases in MgO, Al_2O_3 and CaO, as well as less pronounced K_2O increases and the absence of early TiO_2 enrichments. Maximum Al_2O_3 contents in mafic NLV lavas are lower than in Unit 0 lavas, but they decrease much less markedly towards andesites. Consequently, NLV dacites and andesites have among the highest Al_2O_3 contents for SVZ lavas with comparable SiO_2 wt%.

In addition to differences between NLV and the underlying Unit 0 volcanic rocks, systematic differences can be recognized internally to NLV, from Units 1 to 4. The most noticeable variation is a progressively lower enrichment rate of K_2O and other incompatible elements with time (**Figure 3**). Unit 1 andesites have K_2O contents for a given SiO_2 that are slightly lower than those of Unit 0 and are similar to other volcanoes of the region, whereas Unit 4 is characterized by the lowest K_2O values in the SVZ. Main-cone andesites have intermediate K_2O contents (Unit 3b < Unit 3a). The complete dataset of whole-rock data is presented in the **Supplementary Material S2**.

4.2 Trace Elements

Most incompatible trace elements follow the behavior of K_2O in that their rates of enrichment with increasing SiO_2 systematically decrease from Unit 0 to Unit 4. This tendency is particularly marked for highly incompatible elements such as Rb, Zr, Th, LREE, Nb, Hf, and U (**Figure 4**). Differences in incompatible element concentrations are most significant in intermediate and evolved compositions, but for many elements there are noticeable differences among mafic lavas as well. Incompatible element concentrations are also highly variable in evolved compositions of Unit 3a; i.e., factor of two range for Rb in

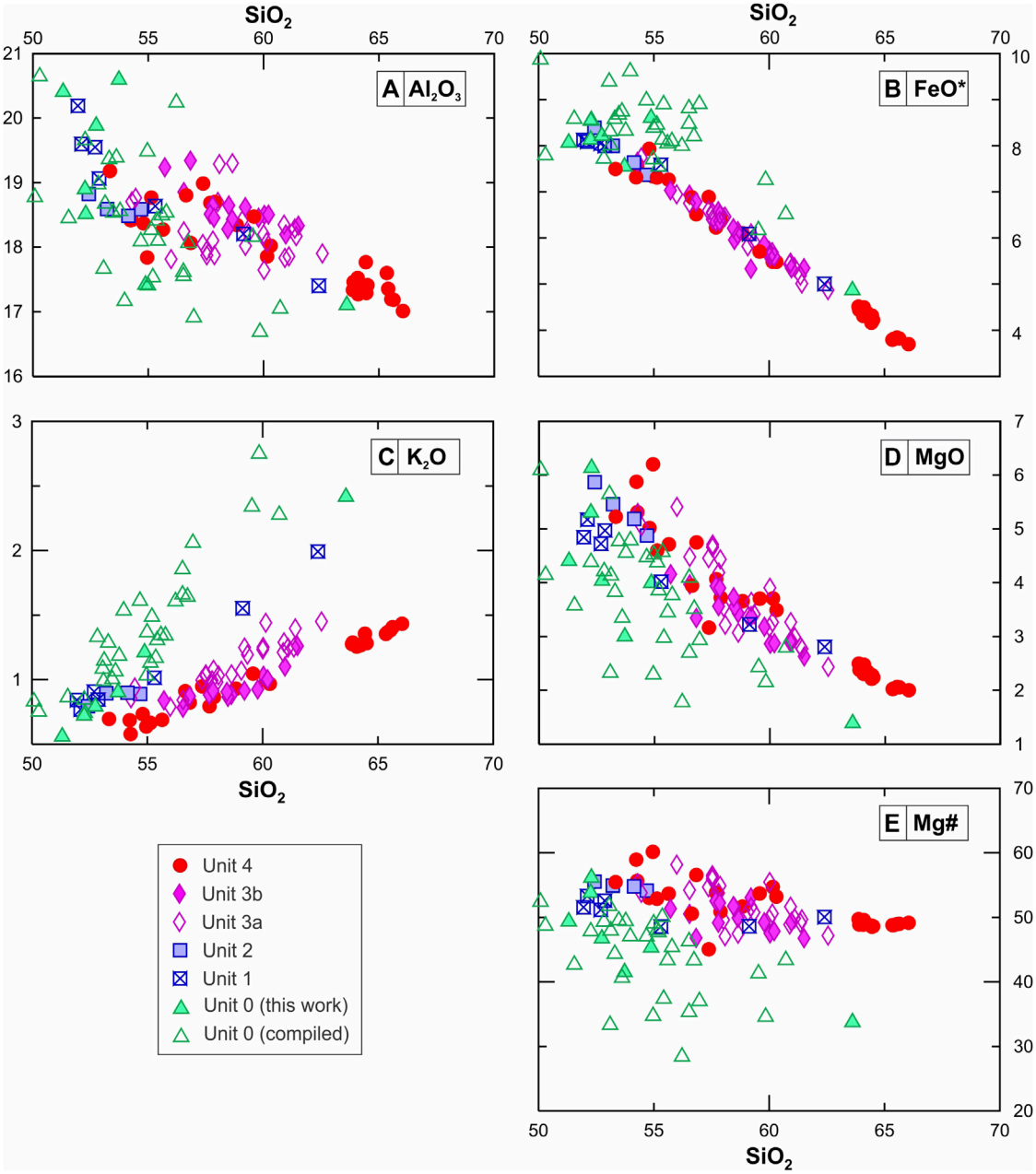

FIGURE 3 | Major element **(A–D)** and $Mg^{\#}$ **(E)** variation of the Pleistocene to Holocene units from Nevado de Longaví volcano. Unit 0 corresponds to the underlying Villalobos volcano. In comparison to Longaví, Al_2O_3 in Villalobos lavas (as well as MgO and CaO) decreases more abruptly, whereas K_2O (and Na_2O) increase more steeply with increasing differentiation. Compiled Unit 0 analyses are from Gardeweg (1980), Muñoz and Niemeyer (1984), and Kay et al. (2006).

andesites with ~57–60 wt% SiO_2. Exceptions to this general pattern are the high Th, U, and Pb values in mafic lavas of Unit 2. Strontium behaves similarly to Al_2O_3, with an overall decreasing trend in basal Units 0 to 2, whereas Units 3a, 3b and 4 feature increasing Sr contents up to a SiO_2 ~57 wt%, which then decrease with further differentiation. Y and HREE contents increase with increasing SiO_2 in Unit 0, remain relatively constant in Units 1–3, and decrease with increasing differentiation in Unit 4. Similar Y and HREE depletions have not been observed at other SVZ centers. Consequently, the La/Yb ratios of Holocene NLV lavas are higher than those at most other SVZ volcanoes. Only lavas from volcanoes in the northernmost SVZ have higher La/Yb, but unlike NLV they are preferentially enriched in La rather than depleted in HREE.

Incompatible fluid-mobile elements, such as Ba and Pb (but also Na_2O, Li, Be, Sb and Cs) show smaller differences among units, whereas boron is systematically higher in younger units, in contrast to the behavior observed in immobile incompatible elements, such as HFSE. Ratios of fluid-mobile to fluid-immobile incompatible elements, such as B/La and Ba/La,

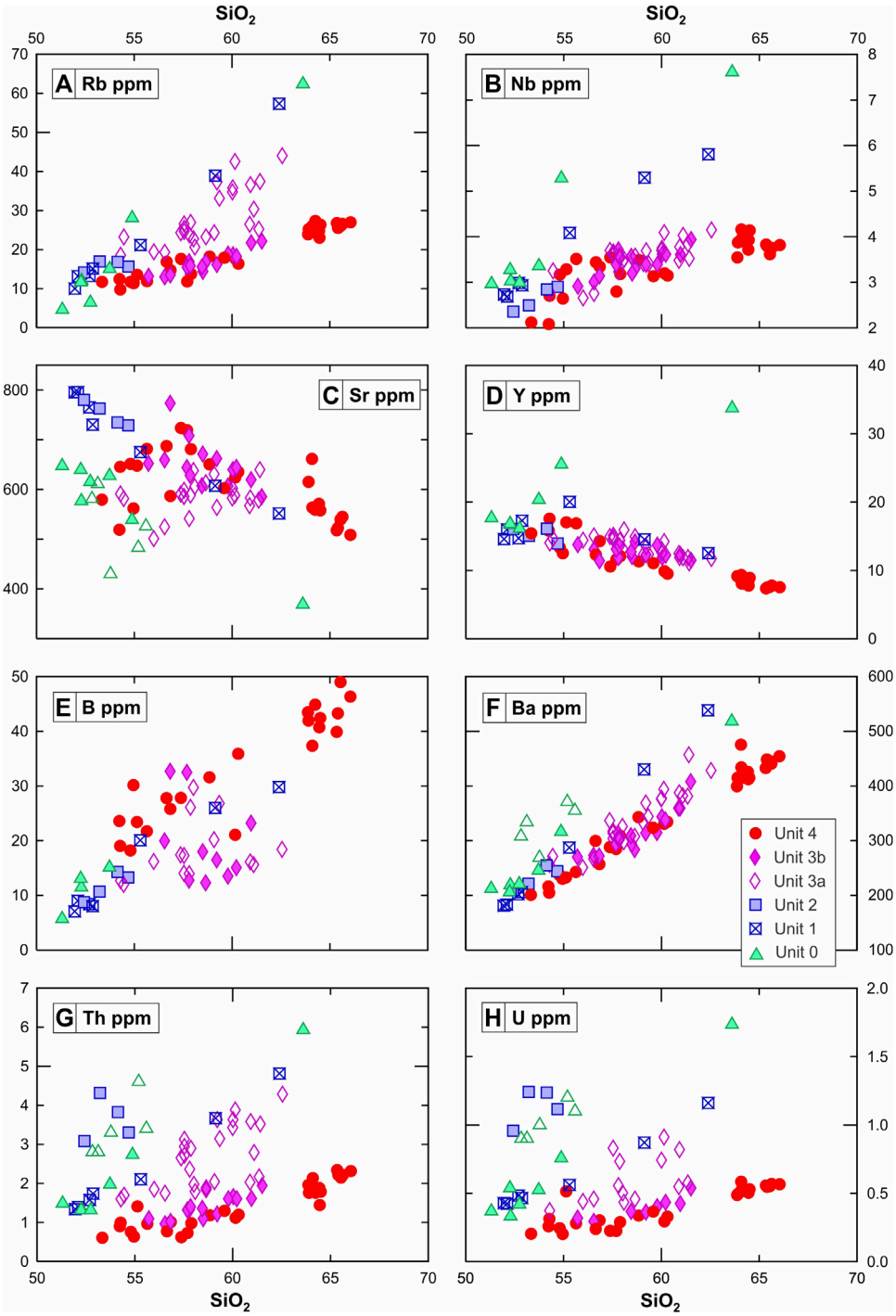

FIGURE 4 | Trace element variations **(A–H)** for the different units defined at Nevado de Longaví. A sustained decrease in incompatible element content (for a given SiO_2 content) from old to young units is clearly seen in Rb, Nb, Th and U (similar to K_2O, Figure 3). Unit 2 lavas have exceptionally high Th, U and Pb contents. Boron shows the opposite tendency of higher contents in younger units. Y decreases with increasing SiO_2 in all Longaví units, but increases among Unit 0 lavas.

remain relatively constant or slightly increase with differentiation within a given unit (**Figure 5**), but change markedly across units. Units 0–2 have Ba/La and B/La ratios that are 30–70% lower than Unit 4 magmas; Units 3a and 3b are more scattered and distributed between the two extremes.

Other ratios of petrogenetic interest further elucidate trends along series and systematic differences among Units (**Figure 5**). Sr/Y decreases with SiO_2 in Unit 0, does not vary significantly in Units 1 and 2, and increases in younger units. Th/La increases slightly within all units, albeit at different starting levels. This

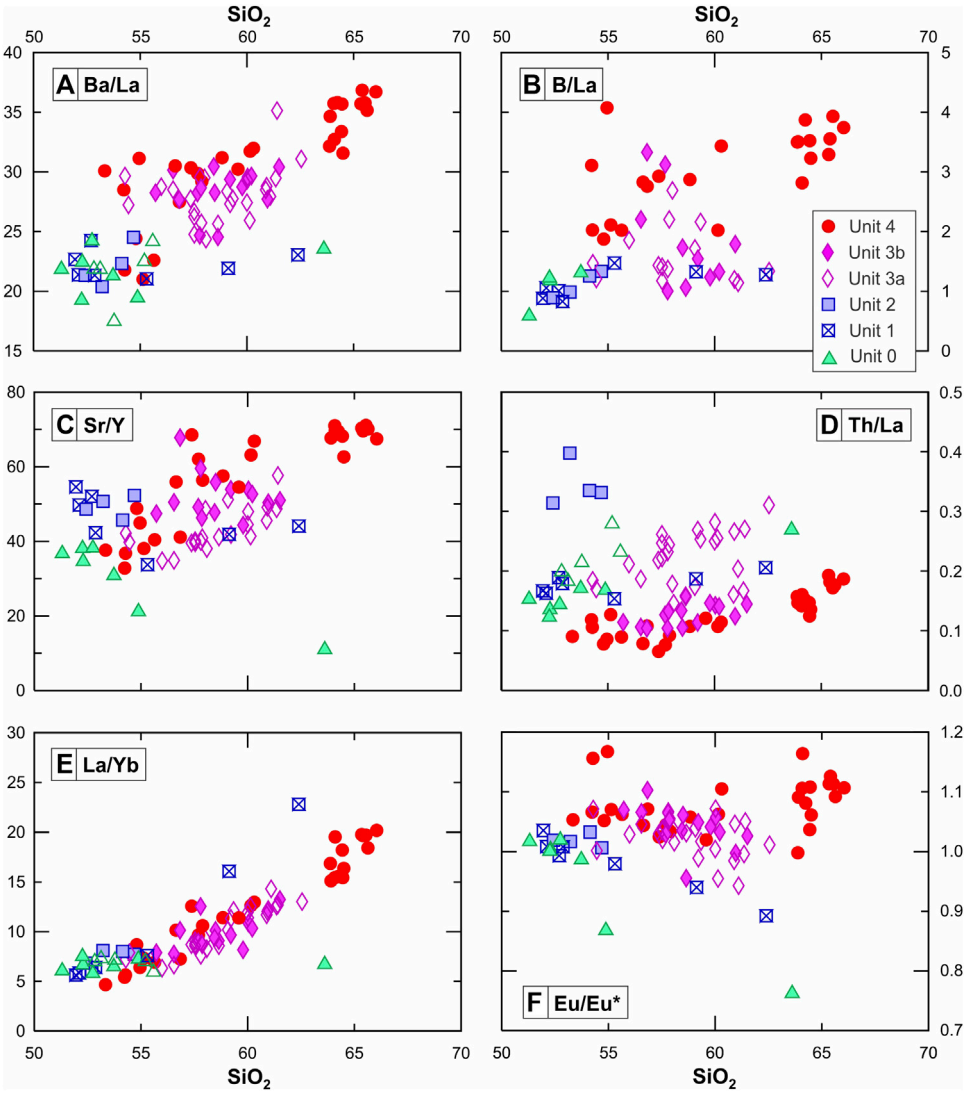

FIGURE 5 | Selected trace element ratios **(A–F)** as a function of silica contents for Longaví and Villalobos magmas.

highlights the unusual mafic composition of Unit 2, which have significantly higher Th/La than other unit (as well as U/La and Pb/La, not shown). La/Yb ratios remain nearly constant at low values (~7) for Units 0–2, except for two more evolved prismatically jointed fragments in Unit 1, which are among the highest values of the set, whereas Units 3a, 3b and 4 increase La/Yb as silica increases. Eu/Eu* values decrease with differentiation in Units 0 to 2, decrease only slightly in Unit 3a, and remain essentially constant in Units 3b and 4.

4.3 Isotopes

The analyzed samples define a relatively narrow range of isotopic compositions for SVZ magmas. NLV isotopic values conform to the regional SVZ along-arc trends in the sense that NLV isotopic data straddle the intersection of the fields defined by the volcanic centers north and south of this latitude (**Figure 6**), with most $^{87}Sr/^{86}Sr$ values around 0.7040. Strontium isotopic ratios remain relatively constant within the defined units across all silica contents, whereas Nd ratios have greater scatter in Units 0 and 1. Samples from Unit 2 have the most "crustal" isotopic signatures, while samples from Unit 1 have lower $^{143}Nd/^{144}Nd$ and $^{87}Sr/^{86}Sr$ Both ratios are within narrow ranges for Units 3a and 4 (0.70392–0.70408 and 0.512749–0.512812). Analytical methods details are provided in the **Supplementary Data Sheet S1**.

5 RESULTS: MINERAL CHEMISTRY

Several thousand data points were collected in order to fully characterize the mineralogy of selected samples from all units. Here we focus on the mineral-chemistry features that are systematically different among units and which correspond to contrasts in magmatic processes that have operated through time.

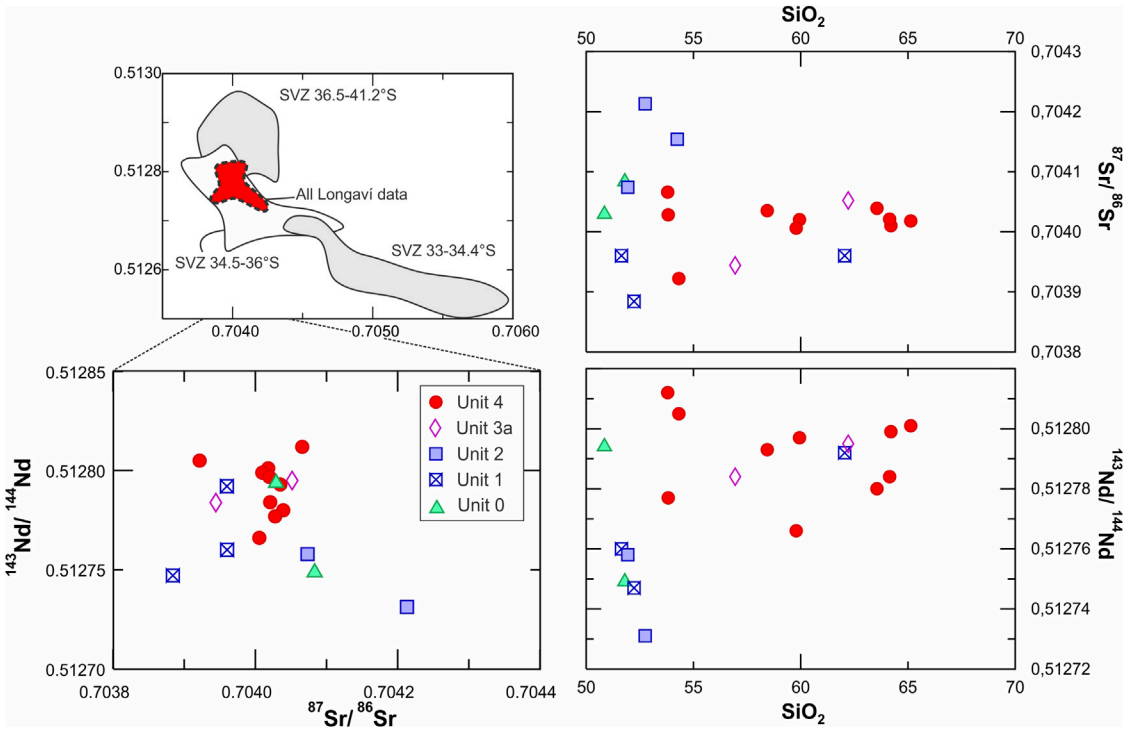

FIGURE 6 | Sr and Nd isotopic composition of Longaví and Villalobos lavas. Fields for other SVZ segments are shown in insert. Analytical error bars are about the size of symbols.

Only a summary of the most relevant results is presented here; for more details the reader is referred to Sellés (2006) and Rodríguez (2006).

A range of plagioclase compositions from An_{90} to An_{03} is recorded in lavas from Villalobos and Longaví volcanoes, with Unit 0 and Unit 1 basalts exhibiting the widest An distributions (**Figure 7**). Marked modes between An_{45} to An_{65} characterize basaltic andesites and andesites from Units 2 and 3, whereas the predominant plagioclase composition in Unit 4 dacites is slightly more sodic (An_{35} and An_{55}). Unit 4 mafic enclaves have a pronounced mode at An_{60-65}.

Olivine is commonly present in mafic lavas from units 0–2, and their compositions are widely distributed between Fo_{60} and Fo_{85}. It is also occasionally found in Unit 3a, it is extremely rare in Unit 3b andesites, and is only present in some Unit 4 mafic enclaves and in hybrid lavas. The narrow range of Mg- and Ni-rich olivine in Unit 4 suggests that olivine only crystallized from mafic liquids, whereas in older magmas it continued to be stable in more evolved compositions.

Most andesites from units 1 to 3 contain both orthopyroxene and clinopyroxene, whereas basalts from Unit 0 contain mostly clinopyroxene. Clinopyroxene is absent from Unit 4 dacites and enclaves. Orthopyroxene in Unit 4 is characterized by relatively low Mg# (67–75) and high Mn contents (typically >0.8, and up to 1.1 wt %). The range of clinopyroxene compositions are similar in all units, although Unit 3b displays limited variability (Mg# 75–85). Unit 3a hosts the most Cr- and Al-rich clinopyroxene analyzed, with values up to 0.9 wt% Cr_2O_3 and 7.5 wt% Al_2O_3. A few analyses from Unit 2 also extend to high Cr and Al values, although the vast majority are restricted to Al_2O_3 < 4 wt% and Cr_2O_3<0.1 wt%, where most pyroxenes from Units 1 and 3b are concentrated. Clinopyroxene in Unit 0 lavas has relatively high Cr_2O_3 contents, but Al_2O_3 is low and comparable to most clinopyroxene analyses from younger units.

Amphibole is the predominant ferromagnesian phase in Holocene NLV dacites and their included enclaves (Unit 4). It is an abundant phase in many main-cone andesitic lavas with SiO_2 as low as 57 wt% (Units 3a and 3b). Andesites from the north basal unit (Unit 2) also contain scarce amphibole phenocrysts, but this phase has not been observed in Units 0 and 1, not even in evolved compositions. Amphiboles in NLV lavas define three compositional groups. High-Al amphiboles (Al_2O_3 > 11 wt%), which classify mostly as Mg-hastingsite (Leake et al., 1997), are common to all amphibole-bearing units (Units 2–4). Mg-hastingsite amphiboles contain appreciable amounts of Cr_2O_3 (up to 1 wt%) and show a wide variation in Mg# (78-58) with nearly constant tetrahedral Si/Al ratio. Amphiboles of this composition form up to 90 vol% of cumulate-textured xenoliths collected in young NLV lavas (Sellés, 2006). Low-Al amphiboles (Al_2O_3 < 10 wt%), which classify mostly as Mg-hornblende, have been found exclusively in Unit 4, mostly in dacites but also as late phases in mafic enclaves. They are characterized by a wide variation in tetrahedral Si/Al ratios, which correlate positively with Mg# and negatively with K. A third group with intermediate Al_2O_3 but higher TiO_2 and K_2O contents than other groups is represented by variably reacted amphibole crystals that commonly contain euhedral plagioclase and/or opx inclusions. Such Ti-edenites and are found

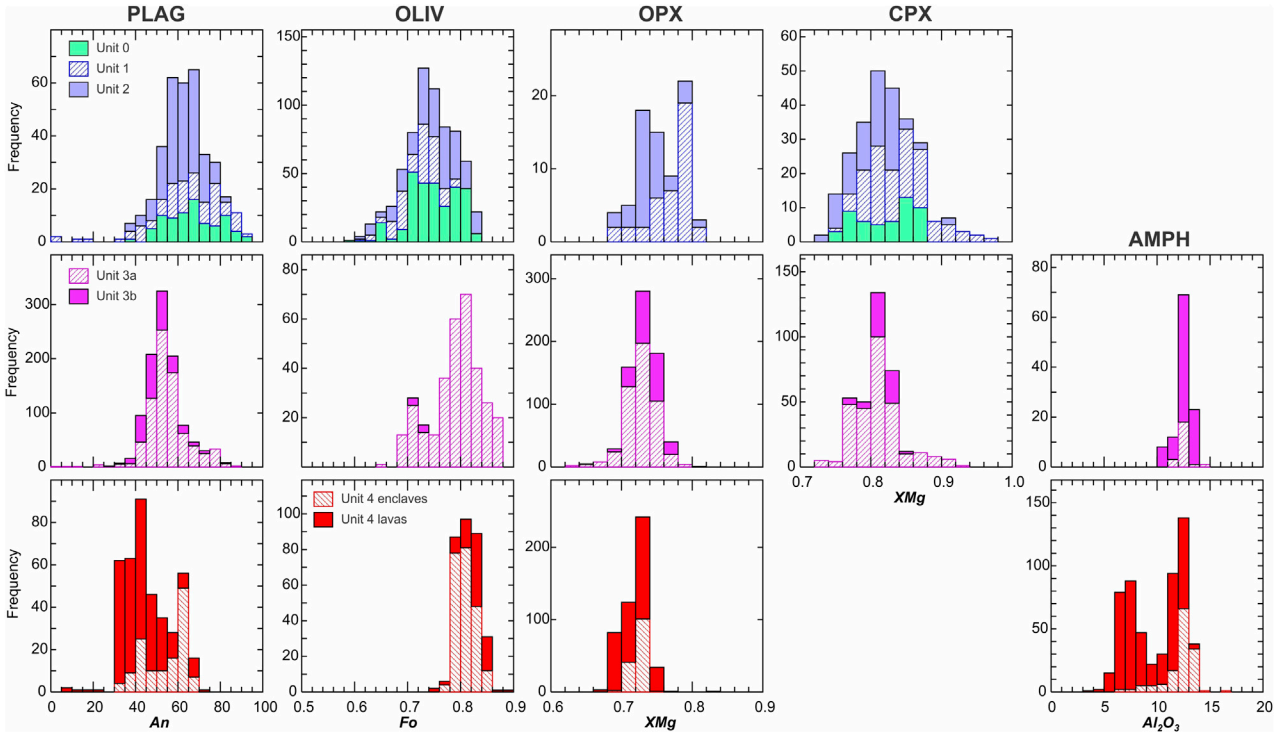

FIGURE 7 | Mineral chemistry histograms by unit.

exclusively in Unit 3a lavas in combination with fresh Mg-hastingsite crystals. They are compositionally and texturally similar to post-cumulus amphiboles in some noritic xenoliths from NLV lavas (Sellés, 2006), and we interpret them as xenocrysts resulting from disaggregation of partially molten xenoliths.

5.1 Fe-Ti Oxides

Temperature and fO_2 were calculated for coexisting Fe-Ti oxide compositions with the methodology described in **Supplementary Material S1**. The results are shown in **Figure 8A** in the form of average values per sample, where individual samples are represented by 1 and up to 54 mineral pairs (detailed analyses are given in **Supplementary Material S3**). Units 0, 1 and 2 are the least oxidized of the dataset, with fO_2 values ranging from 1 log unit below the NNO buffer up to 0.5 units above NNO. Main Cone lavas from Units 3a and 3b cover a range of fO_2 values between NNO-0.5 and NNO+1.2 with significant scatter (large numbers of samples were analyzed). Unit 4 magmas exhibit fO_2 values between NNO+1.25 and NNO+1.7, which, to our knowledge, are the highest fO_2 values reported for this part of the Andes. Magmatic oxidation states at NLV increased by nearly three fO_2 log-units during the Quaternary. Changes in redox state were accompanied by increases in fluid-mobile-to-immobile element ratios (**Figures 8B,C**). The calc-alkaline—tholeiitic index (Hora et al., 2009) also correlates well with oxidation state **Figure 8D**.

6 DISCUSSION

6.1 Evolved NLV Magmas: An Oddity in the SVZ

Nevado de Longaví magmas exhibit some unique chemical and mineralogical characteristics among SVZ magmas. These are best defined by andesitic and more evolved lavas, which are characterized by a combination of elevated fluid-mobile to fluid-immobile element ratios, low incompatible element concentrations and indications of high-pressure fractionation. Trace element ratios commonly used to trace subduction fluid inputs, such as Ba/La, B/La and Sb/La, are higher in NLV Units 3–4 magmas than in other volcanoes of the SVZ. Basal NLV Units 0–2, on the other hand, have Ba/La, B/La and Sb/La that are similar to the values observed along the arc, consistent with the latitudinal variation trends (**Figures 9A–C**). Evolved NLV lavas (SiO_2 >60 wt%), especially Unit 4, display high La/Yb and Sr/Y ratios that require the participation of garnet as a residual phase (Rodríguez et al., 2007). Some magmas erupted to the north of NLV have similar or higher La/Yb and Sr/Y values, but unlike NLV lavas, these are accompanied by the participation of crustal components as is suggested by high $^{87}Sr/^{86}Sr$ and overall high incompatible element contents (**Figures 1C**, **9D**,**E**). Some evolved magmas south of NLV, where crustal assimilation is thought to be less significant, have low incompatible element abundances and less radiogenic $^{87}Sr/^{86}Sr$, but most of the magmatic evolution takes place at low pressure, with no garnet participation (e.g., Gerlach et al., 1988; Hickey-Vargas et al.,

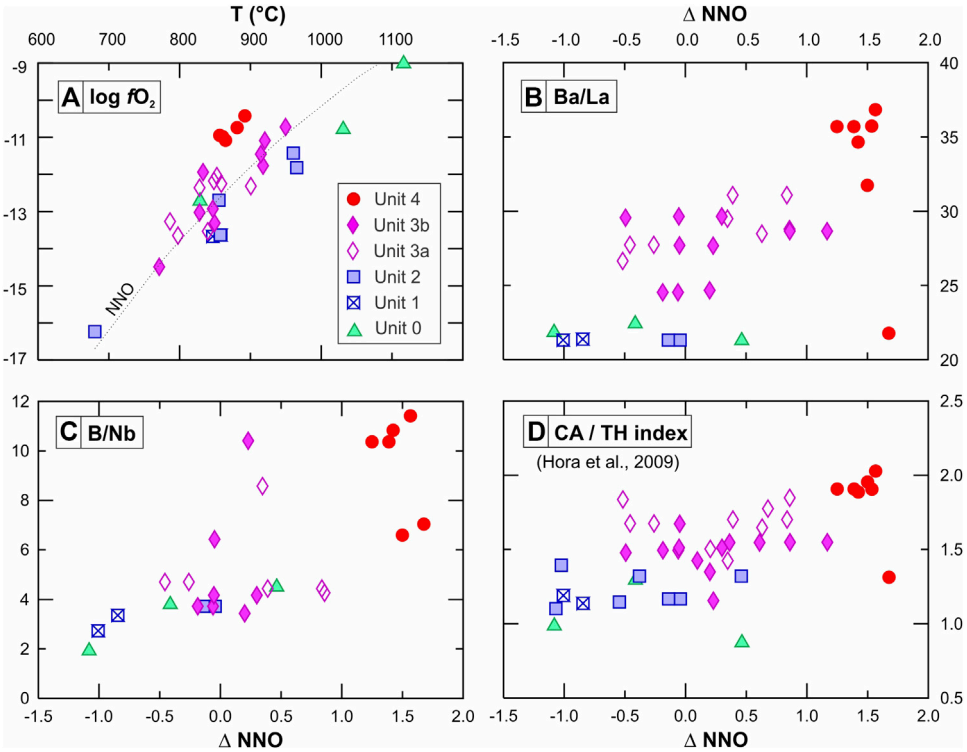

FIGURE 8 | Oxygen fugacity as function of temperatures **(A)** as estimated by coexisting Fe-Ti oxides. NNO refers to the nickel-nickel oxide buffer. Departures from this buffer in log units (ΔNNO) are plotted against subduction fluid indicators (Ba/La, B/Nb; **(B-C)**) and the Calc-alkaline/Tholeiitic index (CA/TH) of Hora et al. (2009) **(D)**.

1989; López-Escobar et al., 1995b). NLV is the sole volcanic system in this portion of the SVZ that has generated evolved magmas with this combination of characteristics (**Figure 9F**).

High abundances of amphibole phenocrysts in NLV lavas are exceptional. Amphibole is the main ferromagnesian phase in Units 4 and 3b, but it also is commonly present in Unit 3a, and less so in Unit 2. No amphibole phenocrysts or relicts have been found in the older Units 0 and 1. Amphibole is also a common phenocryst phase in K_2O-rich evolved lavas north of 36°S, (Hildreth and Moorbath, 1988 and references therein), but it is usually subordinate to anhydrous ferromagnesian phases (Ferguson et al., 1992; Feeley et al., 1998; Sruoga et al., 2005). South of NLV, amphibole has only been found in small amounts in evolved lavas from the Mocho-Choshuenco complex, (39.9°S; McMillan et al., 1989), and from the Pleistocene Tronador volcanic complex (41.2°S; Mella et al., 2005). It is inferred to be an important fractionated phase in andesites from Calbuco volcano (41.3°S; López-Escobar et al., 1995b), and is also present in some andesites and dacites south of this latitude (López-Escobar et al., 1993). In none of these known occurrences, with the remarkable exception of Huequi volcano (42.4°S; Watt et al., 2011), is amphibole as abundant as it is at NLV. Rodriguez et al. (2007) modeled the major and trace element evolution of Unit 4 magmas by fractionation of a mineral assemblage wherein amphibole is the main ferromagnesian phase, and this is further supported by the occurrence of amphibole-rich cumulate xenoliths, some of which contain primary interstitial glass.

What specific factors determine that NLV magmas are unlike other SVZ magmas? Our preferred explanation relies on the role of the subducted Mocha Fracture Zone (MFZ) as the source of high amounts of fluid to the subarc mantle. Oceanic fracture zones are pathways for seawater infiltration, which promotes serpentinization of the oceanic lithosphere. Antigorite, which contains ~10–13 wt% H_2O, persists to high pressures and temperatures in subducted slabs, such that it is a candidate for being a contributor of water-rich fluids to arc magma sources in asthenospheric mantle wedges. If indeed the MFZ is responsible for the particularities of NLV magmas, then its impact on magma generation must have varied through time, as the MFZ is not stationary relative to the continental margin. We focus below on changes in petrology and geochemistry of erupted magmas during the temporal evolution of NLV.

6.2 Closed-System Evolution

Major element mass-balance models were fit to the range of mafic to intermediate compositions in each unit in order to approximate the mineral assemblages that could reproduce the observed trends if differentiation was dominated by closed-system crystal extraction. Details of the models run can be found in the **Supplementary Material S4**. **Figure 10** summarizes the calculated mineral assemblages that best reproduce major element trends for each unit. The mineral assemblage calculated here for Unit 4 differs slightly from the

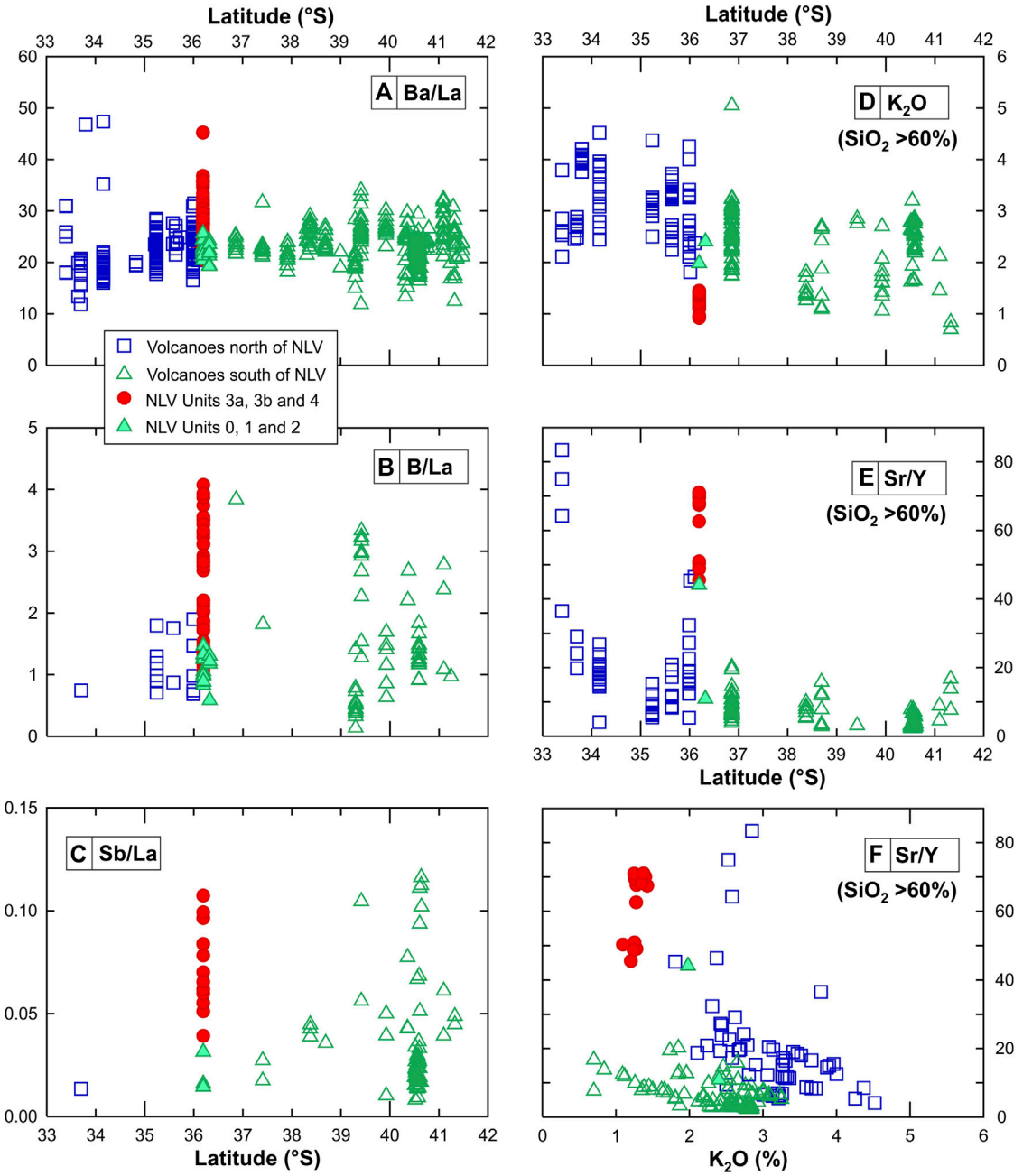

FIGURE 9 | (A–E) Fluid-mobile to fluid-immobile element ratios (all compositions), and K_2O contents and Sr/Y ratios of evolved magmas (SiO_2≥60 wt%) along the SVZ. **(F)** K_2O versus Sr/Y ratios of SVZ magmas with SiO_2≥60 wt%.

one presented by (Rodríguez, et al., 2007) because we have fit the model to the aggregate data trends rather than aiming to match the composition of a particular evolved sample.

Models such as these are simplifications of more complex systems in which mineral proportions and compositions change continuously. The solutions are non-unique, as data scatter allows for some latitude in fitting the model. Such models are not quantitatively rigorous but appear to be sufficiently robust to provide meaningful insights. For example, increasing proportions of amphibole extracted from Unit 2 onwards is (arithmetically) the only way to suppress K_2O-enrichments without causing a large decrease in Mg#. Increasing proportions of amphibole are accompanied by decreases in amounts of fractionated plagioclase, which reproduce the slightly higher Al_2O_3 contents that are typical of NLV magmas (**Figure 3**).

The shift from anhydrous mineral assemblages for Units 0 and 1 to amphibole-rich associations from Unit 2 onwards is consistent with the observed mineralogy. Olivine is the only

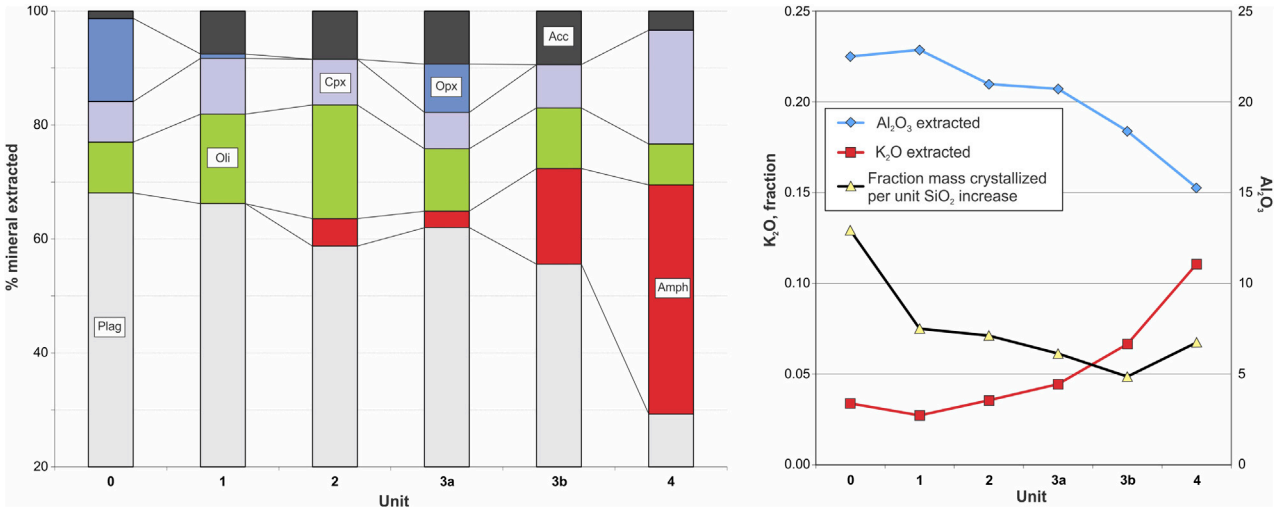

FIGURE 10 | Summary of fractionation model based on major elements. Accessory minerals ("Acc") include the calculated proportions of magnetite, ilmenite and apatite.

major phase that can drive residual liquids to higher silica contents in early units, as both plagioclase and clinopyroxene have SiO_2 contents comparable to those of basaltic liquids (~50 wt%). Olivine proportions in younger units are much lower, and orthopyroxene becomes correspondingly more important. Fractionation of Mg-hastingsitic amphibole (~43 wt % SiO_2) plays a dominant role in raising the SiO_2 of residual magmas in these younger units. The change from olivine-to amphibole-driven differentiation is consistent with young andesites having higher Mg#'s than older, less water-rich magmas (**Figure 3E**).

Fractionation of plagioclase-rich, high-SiO_2 assemblages in Unit 0 lavas resulted in limited silica increases plus rapidly increasing alkalis and decreasing MgO and Al_2O_3 in derivative liquids. These consequences are consistent with the large range of olivine phenocryst compositions recorded in Units 0 and 1. Olivine stability is favored by rapidly increasing K_2O because alkalis have the effect of expanding the olivine primary phase volume (Grove and Juster, 1989; Longhi, 1991). In NLV Units 2 through 4, amphibole-driven differentiation rapidly increases the SiO_2 contents of derivative liquids, thereby favoring crystallization of orthopyroxene rather than olivine, which is consistent with narrow ranges of Fo-rich olivine compositions.

Limited spinel fractionation (<3 wt%) from Unit 0 lavas is consistent with the observed early iron enrichment, and high-temperature ilmenite is required to limit TiO_2. Low proportions of Fe-Ti oxides relative to silicates crystallizing from Unit 0 magmas probably relates to the reduced nature of these magmas (**Figure 8**) and low magmatic water contents (Sisson and Grove, 1993). Spinel proportions are higher for all NLV units (>5 wt%), consistent with increasing water contents and increasing oxygen fugacity, which also has the effect of increasing the oxide saturation temperatures (Pichavant et al., 2002).

Fractionation of significant amounts of amphibole from NLV magmas contributes to low rates of incompatible element enrichments with SiO_2, in part because it lowers bulk silica contents of fractionating mineral assemblages. Also, amphibole more readily accommodates some elements that are highly incompatible with respect to anhydrous phases, thereby increasing bulk partition coefficients and lowering certain elemental enrichments as function of mass fractionation, as exemplified by K_2O in **Figure 10**. Amphibole fractionation is consistent with the high modal abundances of this phase in late NLV lavas, and is corroborated by presumably cogenetic amphibole-rich, cumulate-textured blocks recovered from young lavas (Sellés, 2006; Rodríguez et al., 2007). The high Cr and Mg#'s of some Mg-hastingsites indicate that amphibole is an early phase in the crystallization sequence.

Amphibole in calc-alkaline mafic magmas has been produced experimentally at various pressures under water-rich and water-saturated conditions, either as a liquidus phase or following olivine and augite (Sisson and Grove, 1993; Moore and Carmichael, 1998; Müntener et al., 2001; Pichavant et al., 2002; Grove et al., 2003; Grove et al., 2005). The relationship among experimental amphiboles described by Grove et al. (2005) predicts that the most magnesian amphiboles in NLV (Mg# = 0.78) could have precipitated from mafic magmas with ~9 wt% H_2O.

If the fractionation models advocated here and by Rodríguez et al. (2007) are correct, the minerals that crystallized during the early evolution of Unit 4 magmas have largely disappeared from the nearly aphyric enclave suite. The only surviving phenocryst phase is scarce amphibole-rimmed Fo-rich olivine. The modeled fractionating assemblage requires significant amounts of clinopyroxene and calcic plagioclase that are present in presumably cogenetic amphibole cumulates (Sellés, 2006; Rodríguez et al., 2007), but not in the quenched mafic

enclaves or dacites. Physical separation of phenocrysts may have occurred, but another possible mechanism is that these water-rich magmas became superheated upon adiabatic ascent and crossed the water-undersaturated liquidus (Annen et al., 2006). Superheated water-rich magmas will dissolve the solid phases present, and crystallization resumes only after the water-saturated liquidus is attained. At the point that crystallization resumes amphibole is probably the liquidus phase of Unit 4 enclaves, whereas plagioclase crystallization was suppressed due to high water, and thus highly calcic plagioclase did not crystallize again. Andesitic magmas with 10-7 wt% H_2O are expected to crystallize amphibole at the water-saturated liquidus (Annen et al., 2006).

Garnet is probably among the early phases that did not survive magma ascent. Amphibole fractionation accounts for part of the HREE depletions in NLV evolved magmas, but the steep Y and HREE depletion patterns of Unit 4 mafic magmas suggest that trace amounts of garnet (<2 wt%) could be involved during the evolution of mafic magma (Rodríguez et al., 2007). Amphibole fractionation cannot produce such a pattern because it would require Y and HREE partition coefficients on the order of ~7–8 (assuming amphibole makes ~30–40% of the fractionated assemblage, **Figure 10**), whereas D_Y and D_{HREE} for amphibole in basalts are generally <2 (Dalpé and Baker, 2000 and references therein). Further Y and HREE depletion over the range from 57 to 65 wt% SiO_2 might not require garnet because amphibole partition coefficients increase in silicic liquids. D_Y values of about 6-7 would suffice to explain the observed depletion, which are well within the published valued for silicic liquids (Ewart and Griffin, 1994; Sisson, 1994). Garnet can be a stable phase in hydrous mafic and intermediate magmas at crustal pressures p>~0.8 GPa) as has been experimentally determined (Müntener, et al., 2001; Ulmer and Müntener, 2005; Alonso-Pérez, et al., 2009). This suggests that much of the crystallization of mafic NLV magmas could be taking place in the deep crust (Annen, et al., 2006).

Magmatic evolution seems thus to be primarily the consequence of crystal fractionation, although assimilation of crustal lithologies and magma mixing probably also occurred. The variety of intermediate to evolved magma compositions at NLV is the result of differences in fractionating mineral assemblages and a shift in the composition of the mafic magmas. Both of these effects are consistent with a temporal increase in the water contents of magmas.

6.3 Open-System Processes

Crystal fractionation is probably responsible for many of the distinctive characteristics of NLV lavas. It is unlikely that compositional trends at NLV are related to mixing of silicic crustal melts with mantle-derived basalts, as this would require a silica-rich component with extremely low incompatible element contents. To produce a melt with incompatible element concentrations like those of the Holocene dacites by an acceptably moderate amount of melting (20-5%) would require a source with incompatible element concentrations that were 0.5–0.1 of those in Rudnick and Gao's (2003) estimated lower crustal composition. Even if a purely crustal origin for evolved NLV magmas seems unlikely, evidence for open-system processes is found in many lavas in the forms of disequilibrium textures, partially molten plutonic xenoliths, and mineral chemistry (Sellés, 2006).

Radiogenic isotopes provide few constraints on intra-crustal evolution because of the lack of isotopic contrast with basement lithologies. Comparisons of incompatible element enrichments in evolved and intermediate lavas relative to mafic magmas provide an alternative approach for detecting crustal contributions. This is illustrated in **Figure 11**, showing one or two evolved samples from each unit compared to a trace-element model that assumes the mineral proportions and mass fractions presented above (**Figure 10**), normalized to a mafic sample from the same unit. Details of the modeling process are presented in **Supplementary Material S4**.

Modeled trace element compositions do not differ significantly from natural NLV compositions. The largest mismatch is related to the depletion in HREE in Units 3a and younger, which amphibole extraction alone does not seem capable of reproducing. As shown by Rodríguez et al. (2007), small amounts of garnet (~1%) are required to model this depletion, although it would have negligible impact on the major element budget. Incompatible element enrichments above the modeled compositions, which could indicate open-system inputs such as mixing with crustal partial melts, are modest across NLV Units. Units 0, 1 and 3a do show some departure from predicted patterns, with enrichments in the highly incompatible elements Rb and U, whereas Units 2, 3b and 4 conform to the expected concentrations.

We interpret these patterns as evidence that crustal assimilation plays a relatively minor role in NLV magma evolution, and with a tendency of decreasing influence with time. This tendency of decreasing crustal contamination with time is consistent with magmas being increasingly water-rich and thus colder at crystallization.

6.4 Origin of Mafic Magmas

Intermediate and evolved NLV lavas display a range of compositions that result mainly from fractionation of mineral assemblages that have progressively shifted during the last My from anhydrous (plagioclase dominated) to hydrous (amphibole dominated). These changes in magmatic mineralogy, and associated liquid lines of descent, are consistent with the hypothesis that the MFZ played an increasingly important role as it approaches its current location beneath NLV.

Mafic magmas from Units 0 and 1 that were erupted ~1,000-600 Ka are considered here as reference compositions; i.e. basalts generated with minimum influence from the MFZ, which at the time was 20-12 km further to the north. The trace element systematics of subsequent NLV mafic magmas record variable contributions from two contrasting components. Unit 2 basalts are broadly similar to Unit 0 and 1 compositions, but are strongly enriched in Pb, U, and Th. Enrichment of these elements over La correlate with increasing $^{87}Sr/^{86}Sr$ and $^{206}Pb/^{204}Pb$ and decreasing $^{143}Nd/^{144}Nd$ (see **Figure 12**). These parameters do not correlate with silica or Mg# which suggests that they are controlled more by source processes rather than additions during

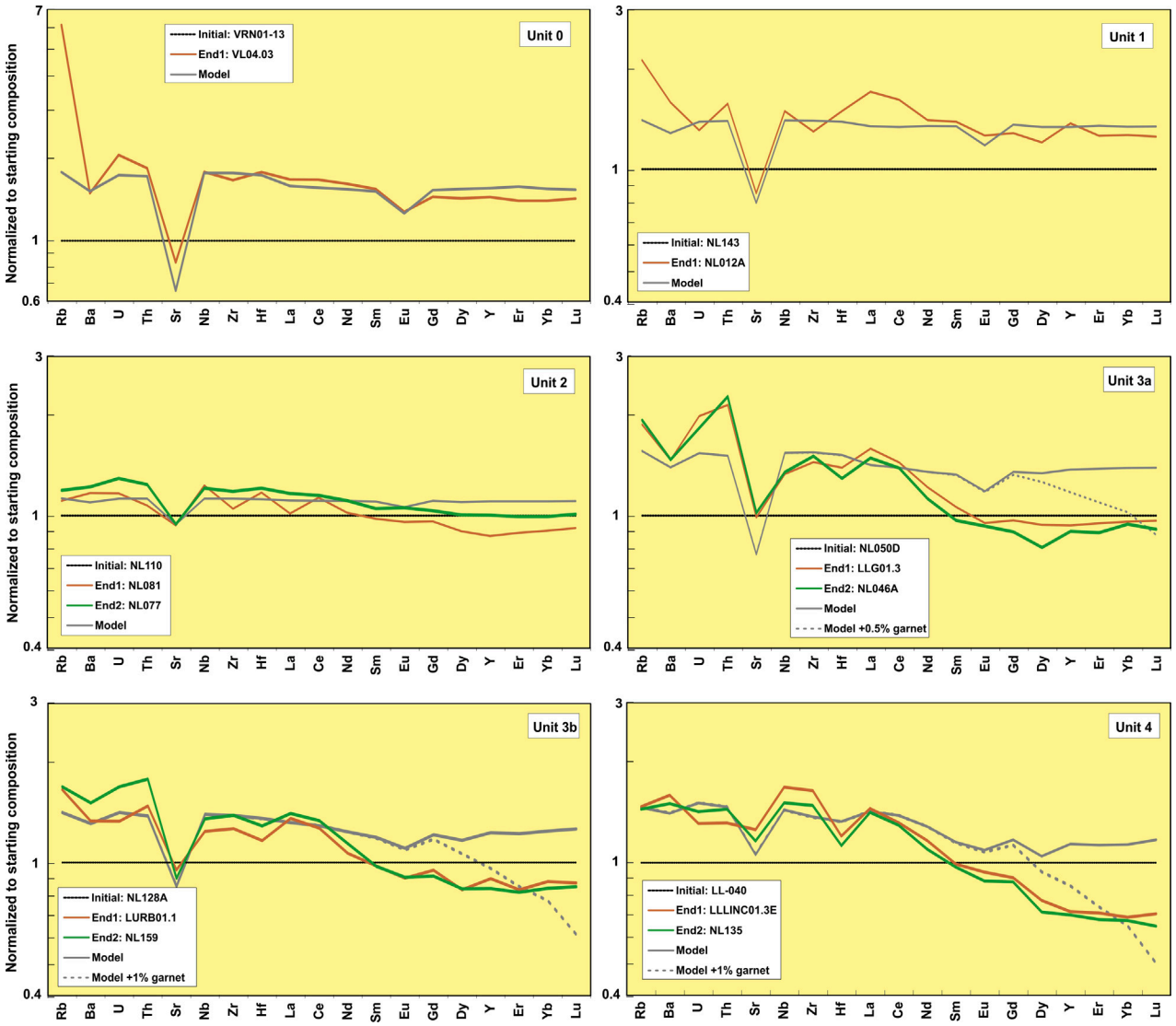

FIGURE 11 | Trace element patterns for natural samples and modeled results.

differentiation/assimilation. Intra-crustal assimilation cannot be ruled out on the basis of these observations alone, but we prefer the hypothesis of source modification, presumably via sediment melts, because we see no evident reason to involve a specific intra-crustal reservoir that contaminates Unit 2 magmas but not previous or later magmas sharing the same ascent paths. A scenario where the subducted components change through time, on the other hand, is a likely consequence of the southward migration of the Mocha FZ. Th and La have similarly low bulk partition coefficients in the context of mantle partial melting. Thus, they will not be fractionated by moderate to large extents of fusion, and the high Th/La signature of Unit 2 is most likely to be inherited from a component other than ambient mantle peridotite. Covariations of Th/La and Sr and Nd isotopic compositions indicate that these elements were to some extent provided by a component with high radiogenic Sr and non-radiogenic Nd. Whereas Pb, Sr, and U might be transported in hydrous subduction zone fluids, Th and Nd are more likely to be efficiently transported in silicic melts. Partial melts of sediments, unlike dehydration-reaction fluids, are enriched in Th, U, and Pb relative to LREE and to other fluid mobile elements like Sr and Ba (Johnson and Plank, 1999). Average Th/La ratio of mafic magmas in several arcs correlate with the mean Th/La of locally subducted sediments (Plank, 2005). These considerations suggest that the high Th/La component in Unit 2 basalts is a silicic melt derived from subducted sediments that was added to the mantle wedge.

Units 3b and 4, on the contrary, have low Th/La ratios that resemble MORB values (<0.1; Plank, 2005), suggesting that the mantle source for these units was not significantly modified by silicic sediment melts. These young units are characterized overall by low abundances of most incompatible elements, but are substantially enriched in B relative to older units (**Figure 4**). Boron is a highly fluid-mobile element that is present in very low

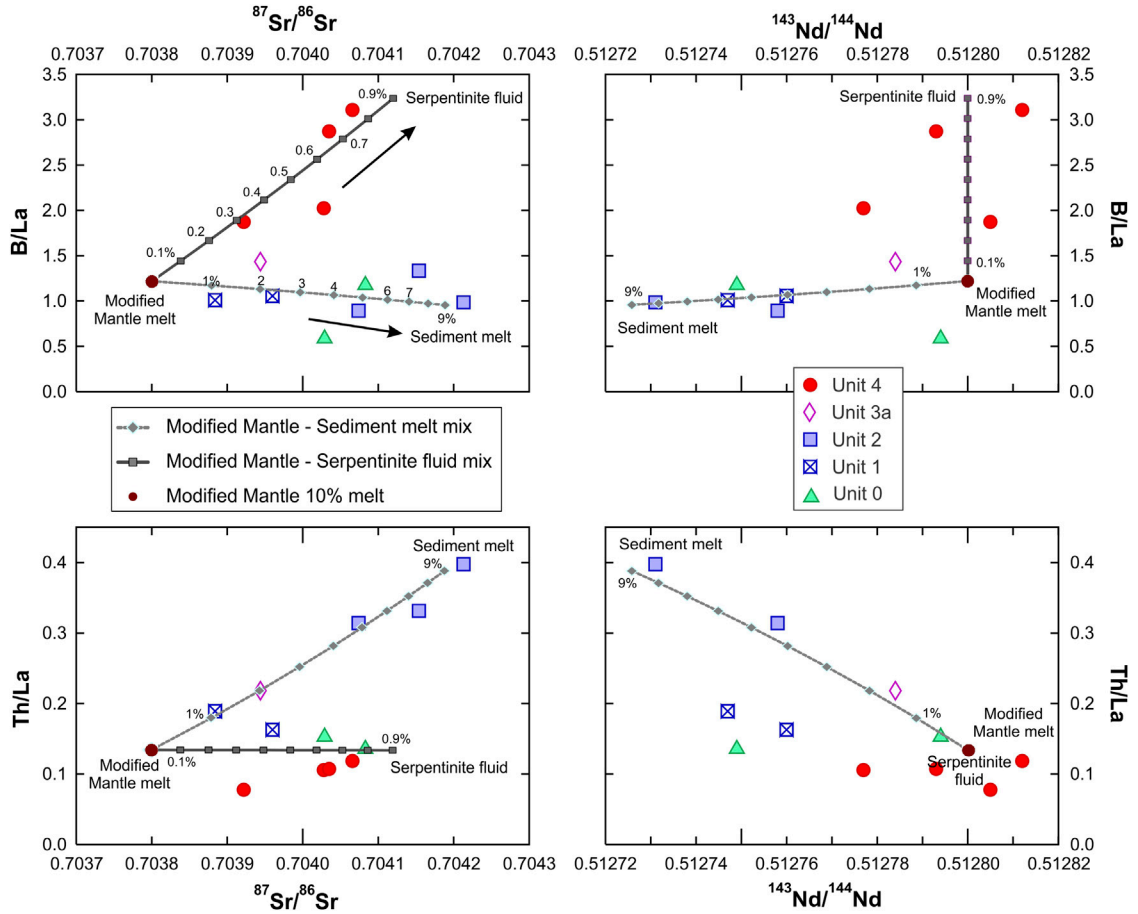

FIGURE 12 | Mixing models between mantle, sediment, and serpentinite components compared to mafic and intermediate NLV samples (SiO_2<60 wt%).

concentrations in the upper mantle (≤~0.1 ppm) and the lower crust (<5 ppm) but is enriched in several lithologies in the subducting plate (sediments, altered oceanic crust, serpentinites; cf. Leeman, 1996). Oceanic sediments can contain high B concentrations (~120 ppm estimated average content for clay-rich pelagic sediments; Leeman, 1996), but as boron is progressively mobilized in fluids liberated during dehydration reactions at shallow depths, contributions of boron from sediments at subarc pressures are diminished (Rüpke et al., 2002). Altered oceanic crust is an important source of elevated B in arc magmas relative to MORBs and OIBs, but the B-inventory is largely dominated by serpentine-derived fluids when deep-seated serpentinitic bodies are present in the oceanic lithosphere (Tenthorey and Hermann, 2004). Other fluid-mobile trace elements are also enriched in the young NLV units relative to older magmas, and they variably correlate with B/La. Ratios such as Cs/La, Li/La, Ba/La, and specially Sb/La show strong positive correlations with B/La and distinguish younger from older units (with a few outlier exceptions; **Figure 13**). Other commonly used fluid proxies, such as Pb/La, U/Th, and $^{87}Sr/^{86}Sr$, although positively correlated with B/La in Units 4 and 3b, do not attain values higher than those in older, apparently dryer units. This indicates that, although the fluid mobility of Pb, U, and Sr is not denied, the fluid component involved has lower concentrations of these elements as compared to other components potentially involved in subduction zone magma genesis. Pb enrichments are significantly higher in magmas with participation of sediment melts than in those dominated by dilute fluids.

To model the effect of different fluid components added to the mantle, we have taken the components calculated by Singer et al. (2007) as a starting point. Singer et al. (2007) documented the geochemical characteristics of Seguam volcano, in the Aleutian arc, which lies above the projection of the Amlia Fracture Zone. Seguam mafic magmas have lower concentrations of incompatible elements (including the lowest average Th-contents), higher $^{87}Sr/^{86}Sr$, and high fluid-tracer ratios such as B/La, B/Nb, Li/Y, and Cs/La relative to other volcanoes along the arc. These features were modeled as mixing of a modified mantle component and a slab-derived fluid (a mixture of altered oceanic crust and sediment fluids), although Singer et al. (2007) did not specify the participation of serpentinite-derived fluids. This is important, as altered oceanic crust and sediments are

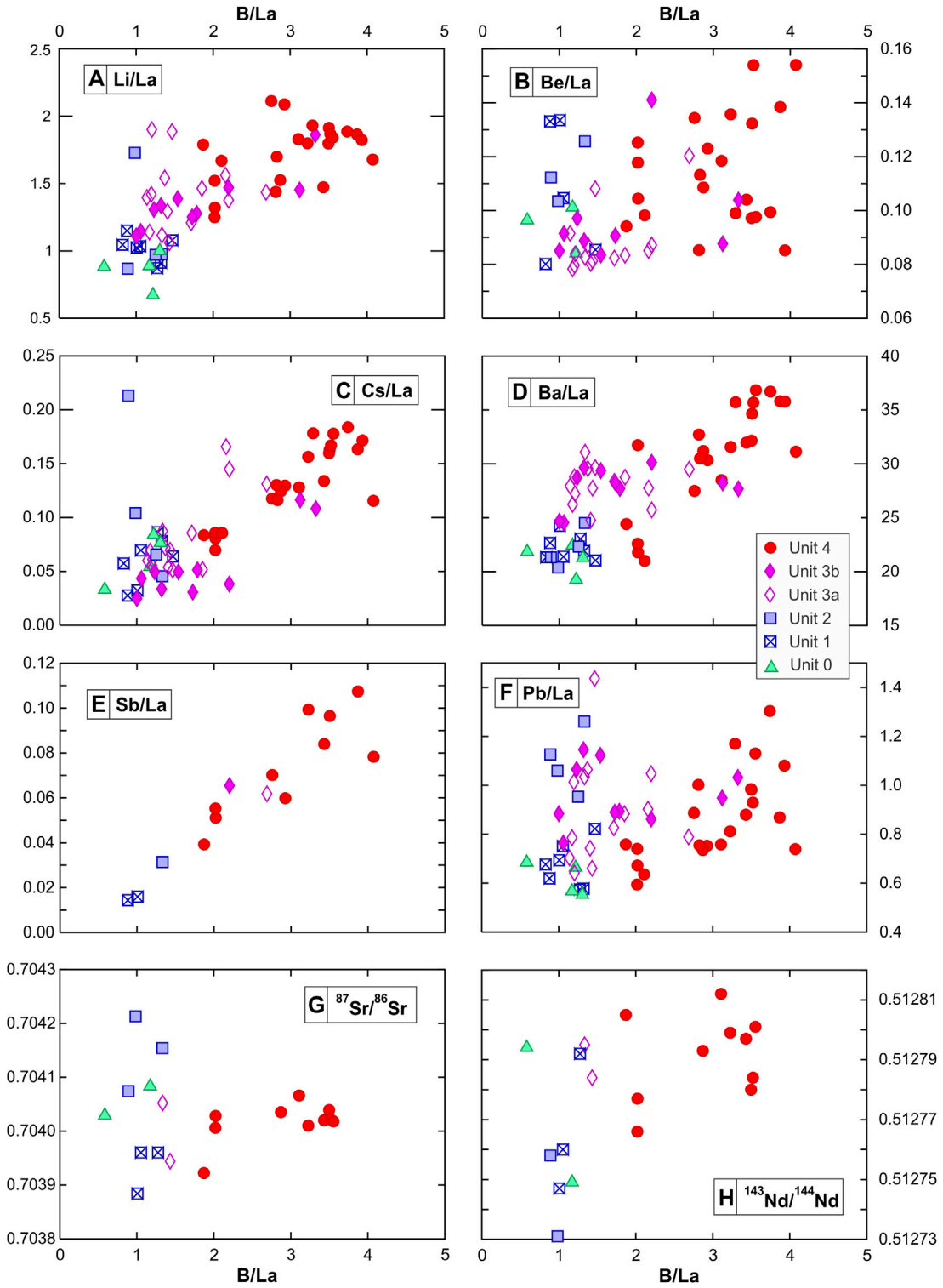

FIGURE 13 | Variation of several fluid-mobile to fluid-immobile element ratios compared to B/La **(A–F)**. Sr and Nd isotopes are also shown **(G–H)**.

components that participate, albeit to varying degrees, all along this and other arcs, whereas serpentinite bodies, especially if associated with fracture zones, exert a highly localized influence.

To approximate the composition of fluids liberated from serpentinitic bodies, we used the fluid/residue partition coefficients experimentally determined by Tenthorey and

TABLE 1 | Values used for models shown in **Figure 12**.

	Sediment melt[a]	Modified mantle[b]	Modified mantle, 10% melt[c]	Serpentinite fluid[d]
B	5.0	1.0	9.1	184.6
La	7.51	0.82	7.93	0.74
Th	5.02	0.11	1.03	0.06
Th/La	0.932	0.134	0.130	0.075
B/La	0.01	1.22	1.14	249.60
Sr	356.9	28.3	256.0	294.7
$^{87}Sr/^{86}Sr$	0.7045	0.7038	0.7038	0.7075
Nd	9.00	1.51	13.46	0.03
$^{143}Nd/^{144}Nd$	0.51260	0.51280	0.51280	0.51280

[a]*From Singer et al. (2007), except B (set to higher value, loosely constrained in source table), $^{87}Sr/^{86}Sr$ (river-mouth sediment value at this latitude, (Hildreth and Moorbath, 1988), and Nd (set to 2x value).*

[b]*From Singer et al. (2007), except B (set to slightly higher value such that melt has B contents comparable to typical SVZ, basalts; Leeman, unpublished), $^{87}Sr/^{86}Sr$ (comparable to lowest values in the SVZ), and $^{143}Nd/^{144}Nd$ (set to highest value of nearby SVZ, volcanoes).*

[c]*Calculated with bulk partition coefficients and mantle modal composition (0.6 ol, 0.3 opx, 0.1 cpx) as in Stolper and Newman (1994). D_B, calculated from mineral/melt coefficients in Brenan, et al. (1998).*

[d]*Calculated assuming 10% fluid liberated from serpentinites with the bulk composition and partition coefficients in Tenthorey and Hermann (2004). $^{87}Sr/^{86}Sr$ estimated assuming 3/4 of Sr from seawater alteration at 0.709 + 1/4 Sr from depleted mantle at 0.7027 (Farley et al., 1993).*

Hermann (2004), assuming 10% H_2O is liberated (coefficients not reported in their Table 1 were estimated from their Figure 4). These coefficients were applied to the bulk serpentinite composition given by Tenthorey and Hermann (2004) in their supplementary table, and the results are presented in **Table 1**.

A mixture of this component and the modified mantle component determined by Singer et al. (2007) adequately reproduces the trend towards high B/La and low Th/La of young NLV units, with up to 1% of the serpentinite fluid component. This mixing of components also explains the variation in Sr isotopic ratios, given that the serpentinites inherit to a great extent the isotopic signature of seawater (**Table 1**). Unit 2 magmas, on the other hand, follow along a mixing line between a mantle and ~9% of a sediment melt component (**Figure 12**). These proportions are however very sensitive to the initial compositions of modified mantle and incoming sediments. The composition of sediments being subducted in this part of the Andes is largely unconstrained, but available data indicate that sediments in the continental shelf are richer in U (3–4 ppm; McManus, 2006) than sediments of the Aleutian trench, consistent with the Chilean Andes being built on continental crust.

An increased flux of slab-derived fluids into the mantle wedge would lead to increasing degrees of melting if other parameters remained constant (notably temperature), because the extent of mantle melting is a strong function of the amount of water present as long as clinopyroxene is not completely consumed (Stolper and Newman, 1994; Hirschmann et al., 1999). Derivation of NLV mafic magmas from progressively higher degree mantle melts is consistent with observed major and trace element characteristics. Hydrous peridotite melts have higher SiO_2 contents (on a volatile-free basis) than anhydrous melts at the same P-T conditions (Hirose and Kawamoto, 1995; Gaetani and Grove, 1998), and for a given temperature, increasing degrees of melting produce liquids with increasing SiO_2 and decreasing Al_2O_3 contents (Hirose and Kawamoto, 1995; Hirose, 1997). Such differences in melt composition reflect expansion of the olivine stability field with increasing water (Ulmer, 2001), which leads to a high pyroxene/olivine contribution to silicate liquids during hydrous melting. High SiO_2 in the most magnesian Unit 4 mafic enclaves may reflect, in part, a primary feature of the primitive magma from which they are derived rather than early fractionation. High-degree partial melts would also be consistent with the low concentrations of incompatible elements observed in Unit 4 mafic magmas, despite their relatively high silica contents.

A causal link between the MFZ and the chemical peculiarities of NLV magmatism is consistent with the highly localized occurrence of these magmas both in space and time. Holocene dacites from the Tatara-San Pedro Complex (TSPC; Dungan et al., 2001), which also currently lies ~35 km further to the northeast and above the projection of the MFZ, tend to share, although in a less pronounced way, some of the chemical characteristics of NLV dacites. Moreover, Holocene TSPC dacites are shifted towards higher La/Yb and Sr/Y and lower K_2O contents relative to pre-Holocene magmas with the same SiO_2 content (**Figure 9**). Further south, Villarica and Osorno volcanoes, located above the projections of the Valdivia and Chiloe Fracture Zones, respectively (**Figure 1**), although lacking evolved compositions, tend to have modestly elevated Ba/La and B/La ratios (**Figure 9**).

The increasingly hydrous nature of magmas produced at NLV correlate with a sustained increase in oxygen fugacity (**Figure 8**). This association of fluid signature and oxidation state of magmas has been observed in regional comparisons among arcs through different proxies and approximations (Kelley and Cottrell, 2009; Evans et al., 2012; Zhang et al., 2021), although there is little consensus on the nature of the processes that link hydrous fluids to oxidation state. Proposed mechanisms range from direct supply of Fe^{3+} and other oxidizing agents from the oceanic crust and sediments to the asthenospheric mantle (Mungall, 2002), to H_2O dissociation into O_2 and H^+, with either degassing or capture of the latter into mineral phases, to preferential removal of Fe^{2+} by fractionating phases. The data collected at NLV does not provide arguments for or against a specific process but constitute a case where the general geodynamic context remains constant while the subduction inputs change over time.

Our model for high Sr/Y magmas at NLV may contribute to the discussion about the origin of an important group of adakite-

like magmas: those associated with porphyry Cu deposits. Adakite-like magmas are found in most major porphyry copper deposits, and in many cases, they can be shown to be contemporaneous and causative of the mineralization. These magmas are known to be hydrous and oxidized, have elevated fluid-mobile to fluid-immobile element ratios, although this is often obscured by hydrothermal alteration, and are usually amphibole-bearing (Richards, 2015; Sun et al., 2015). Low incompatible element contents have not, to our knowledge, been described as a distinctive characteristic of porphyry-related magmas in the literature, but our own survey of published data on Andean porphyries indicates that fertile porphyries tend to exhibit relatively low concentrations, similar to those of NLV dacites. Compressive tectonic regimes are commonly cited as an important factor controlling the fertility of magmas by trapping evolving magmas at depth (Loucks, 2021), but the mechanism(s) by which they become hydrated and oxidized are less consensual. We speculate that regional-scale increases in the amount of slab serpentinization result from plate coupling during tectonic events as a result of increased trench outer-rise bending (Ranero, 2004; Contreras-Reyes et al., 2008). Unlike NLV, which responds to a point-like intersection of a structure with the arc axis, regional-scale enhanced serpentinization would result in increased fluid supplies, more or less simultaneously, along an entire arc segment.

7 CONCLUSION

There are systematic variations in the nature of the magmatism in the area of Nevado de Longaví volcano during the Quaternary, from mainly basaltic, tholeiitic, relatively dry and reduced during the early Pleistocene to very hydrous and oxidized during the Holocene. These variations are manifested on major-element differentiation trends, phenocryst assemblages, trace element concentrations, and oxidation state. Units of intermediate age (3a-3b) are intermediate in character, yet the internal trends follow the overall progression. Most of these variations are consistent with magmas becoming progressively more hydrous with time. Young volcanics from NLV are very different from their precursors and distinct from other magmas in the Quaternary arc. We infer that a local factor is controlling the generation of water-rich melts in the asthenosphere, and that this is first manifested during the Quaternary. We argue that the subducted segment of the oceanic Mocha Fracture Zone is a potentially efficient water supplier to the magmatic source region.

The 1 Ma to present sequence of volcanic rocks studied records a long-term change in the nature of the magmas erupted in the area. This change is recorded in the whole-rock composition of mafic to evolved magmas as well as in the chemistry of the mineral phases present in them. The oldest rocks studied (Villalobos volcano), which are relatively water-poor and reduced, fall within the regional along-arc variation trends represented by most SVZ volcanic centers. Conversely, the youngest erupted rocks are water-rich and oxidized magmas that do not conform to regional trends. The passage from "normal" to "anomalous" magma compositions appears to have been transitional as is attested by units with intermediate ages.

The evolution towards intermediate and evolved magmas is dominated by crystal fractionation of solid assemblages that include increasing amounts of amphibole and lesser proportions of plagioclase with decreasing age, in agreement with the observed phase proportions. Trace element enrichments indicative of open-system processes such as crustal assimilation are more important in old than in young units. Subducted sediments are an important component of one of the early units of NLV.

The observed systematic changes along the stratigraphic section indicate a long-term increase in the proportion of fluid components that fluxed the mantle source. The potentially dominant source of such fluids is serpentinized oceanic mantle within the Mocha Fracture Zone. We conclude that the available data are consistent with an increasingly important role played by fluids from serpentinite dehydration as a consequence of the southward migration of the fracture zone.

DATA AVAILABILITY STATEMENT

The original contributions presented in the study are included in the article/**Supplementary Material**, further inquiries can be directed to the corresponding author.

AUTHOR CONTRIBUTIONS

DS prepared the manuscript and figures. MD performed microprobe analyses in Oregon, guided DS's PhD and participated in the generation of ideas presented. CL and WL provided access to analytical labs to generate data reported in the paper. AR contributed with data and ideas from her PhD. All authors participated in editing and proofreading.

SUPPLEMENTARY MATERIAL

The Supplementary Material for this article can be found online at: https://www.frontiersin.org/articles/10.3389/feart.2022.846997/full#supplementary-material

REFERENCES

Alonso-Pérez, R., Müntener, O., and Ulmer, P. (2009). Igneous Garnet and Amphibole Fractionation in the Roots of Island Arcs: Experimental Constraints on Andesitic Liquids. *Contrib. Mineral. Petrol.* 157, 541–558. doi:10.1007/s00410-008-0351-8

Annen, C., Blundy, J. D., and Sparks, R. S. J. (2006). The Genesis of Intermediate and Silicic Magmas in Deep Crustal Hot Zones. *J. Pet.* 47 (3), 505–539. doi:10.1093/petrology/egi084

Bacon, C. R. (1986). Magmatic Inclusions in Silicic and Intermediate Volcanic Rocks. *J. Geophys. Res.* 91 (B6), 6091–6112. doi:10.1029/jb091ib06p06091

Bohm, M., Lüth, S., Echtler, H., Asch, G., Bataille, K., Bruhn, C., et al. (2002). The Southern Andes between 36° and 40°S Latitude: Seismicity and Average Seismic Velocities. *Tectonophysics* 356 (4), 275–289. doi:10.1016/s0040-1951(02)00399-2

Brenan, J. M., Neroda, E. C., Lundstrom, H. F., Ryerson, F. J., and Phinney, D. L. (1998). Behaviour of boron, Beryllium, and Lithium during Melting and Crystallization: Constraints from mineral-melt Partitioning Experiments. *Geochimica et Cosmochimica Acta* 62 (12), 2129–2141. doi:10.1016/s0016-7037(98)00131-8

Contreras-Reyes, E., Grevemeyer, I., Flueh, E. R., Scherwath, M., and Bialas, J. (2008). Effect of Trench-Outer Rise Bending-Related Faulting on Seismic Poisson's Ratio and Mantle Anisotropy: a Case Study Offshore of Southern Central Chile. *Geophys. J. Int.* 173 (1), 142–156. doi:10.1111/j.1365-246X.2008.03716.x

Costa, F., and Singer, B. S. (2002). Evolution of Holocene Dacite and Compositionally Zoned Magma, Volcan San Pedro, Southern Volcanic Zone, Chile. *J. Pet.* 43 (8), 1571–1593. doi:10.1093/petrology/43.8.1571

Dalpé, C., and Baker, D. R. (2000). Experimental Investigation of Large-Ion-Lithophile-Element-, High-Field-Strength-Element and Rare-Earth-Element-Partitioning between Calcic Amphibole and Basaltic Melt: the Effects of Pressure and Oxygen Fugacity. *Contrib. Mineralogy Pet.* 140, 230–250. doi:10.1007/s004100000181

Déruelle, B., and López-Escobar, L. (1999). Basaltes, andésites, dacites et rhyolites des stratovolcans des Nevados de Chilian et de l'Antuco (Andes méridionales): Ia remarquable illustration d'une différenciation par cristallisation fractionnée. *Comptes Rendus de l'Académie des Sci. - Ser. IIA - Earth Planet. Sci.* 329, 337–344. doi:10.1016/s1251-8050(00)88584-5

Dungan, M. A., Wulff, A., and Thomson, R. (2001). Eruptive Stratigraphy of the Tatara-San Pedro Complex, 36degreesS, Southern Volcanic Zone, Chilean Andes: Reconstruction Method and Implications for Magma Evolution at Long-Lived Arc Volcanic Centers. *J. Pet.* 42 (3), 555–626. doi:10.1093/petrology/42.3.555

Evans, K. A., Elburg, M. A., and Kamenetsky, V. S. (2012). Oxidation State of Subarc Mantle. *Geology* 40 (9), 783–786. doi:10.1130/g33037.1

Ewart, A., and Griffin, W. L. (1994). Application of Proton-Microprobe Data to Trace Element Partitioning in Volcanic Rocks. *Chem. Geology.* 117 (1-4), 251–284. doi:10.1016/0009-2541(94)90131-7

Farley, K. A., Basu, A. R., and Craig, H. (1993). He, Sr and Nd Isotopic Variations in Lavas from the Juan Fernandez Archipelago, SE Pacific. *Contr. Mineral. Petrol.* 115 (1), 75–87. doi:10.1007/bf00712980

Feeley, T. C., Dungan, M. A., and Frey, F. A. (1998). Geochemical Constraints on the Origin of Mafic and Silicic Magmas at Cordón El Guadal, Tatara-San Pedro Complex, central Chile. *Contrib. Mineralogy Pet.* 131 (4), 393–411. doi:10.1007/s004100050400

Ferguson, K. M., Dungan, M. A., Davidson, J. P., and Colucci, M. T. (1992). The Tatara-San Pedro Volcano, 36 S, Chile: A Chemically Variable, Dominantly Mafic Magmatic System. *J. Pet.* 33, 1–43. doi:10.1093/petrology/33.1.1

Folguera, A., Ramos, V. A., Hermanns, R. L., and Naranjo, J. A. (2004). Neotectonics in the Foothills of the Southernmost central Andes (37°–38°S): Evidence of Strike-Slip Displacement along the Antiñir-Copahue Fault Zone. *TectonicsTC5008* 23, 5001–5023. doi:10.1029/2003tc001533

Futa, K., and Stern, C. R. (1988). Sr and Nd Isotopic and Trace Element Compositions of Quaternary Volcanic Centers of the Southern Andes. *Earth Planet. Sci. Lett.* 88 (3-4), 253–262. doi:10.1016/0012-821x(88)90082-9

Gaetani, G. A., and Grove, T. L. (1998). The Influence of Water on Melting of Mantle Peridotite. *Contrib. Mineralogy Pet.* 131 (4), 323–346. doi:10.1007/s004100050396

Gardeweg, M. (1980). Geología del área del Nevado de Longaví. *Cordillera de Los Andes - VII Región Del. Maule.* Memoria de Título, Universidad de Chile.

Gerlach, D. C., Frey, F. A., Moreno-Roa, H., and López-Escobar, L. (1988). Recent Volcanism in the Puyehue--Cordon Caulle Region, Southern Andes, Chile (40 5 S): Petrogenesis of Evolved Lavas. *J. Pet.* 29 (2), 333–382. doi:10.1093/petrology/29.2.333

Grove, T. L., Baker, M. B., Price, R. C., Parman, S. W., Elkins-Tanton, L. T., Chatterjee, N., et al. (2005). Magnesian Andesite and Dacite Lavas from Mt. Shasta, Northern California: Products of Fractional Crystallization of H2O-Rich Mantle Melts. *Contrib. Mineral. Petrol.* 148 (5), 542–565. doi:10.1007/s00410-004-0619-6

Grove, T. L., Elkins-Tanton, L. T., Parman, S. W., Chatterjee, N., Mntener, O., and Gaetani, G. A. (2003). Fractional Crystallization and Mantle-Melting Controls on Calc-Alkaline Differentiation Trends. *Contrib. Mineralogy Pet.* 145 (5), 515–533. doi:10.1007/s00410-003-0448-z

Grove, T. L., and Juster, T. C. (1989). Experimental Investigations of Low-Ca Pyroxene Stability and Olivine-Pyroxene-Liquid Equilibria at 1-atm in Natural Basaltic and Andesitic Liquids. *Contr. Mineral. Petrol.* 103, 287–305. doi:10.1007/bf00402916

Grove, T., Parman, S., Bowring, S., Price, R., and Baker, M. (2002). The Role of an H2O-Rich Fluid Component in the Generation of Primitive Basaltic Andesites and Andesites from the Mt. Shasta Region, N California. *Contrib. Mineral. Petrol.* 142 (4), 375–396. doi:10.1007/s004100100299

Harmon, R. S., Barreiro, B. A., Moorbath, S., Hoefs, J., Francis, P. W., Thorpe, R. S., et al. (1984). Regional O-, Sr-, and Pb-Isotope Relationships in Late Cenozoic Calc-Alkaline Lavas of the Andean Cordillera. *J. Geol. Soc.* 141, 803–822. doi:10.1144/gsjgs.141.5.0803

Herron, E. M. (1981). "Chile Margin Near Lat. 38°S: Chile Margin Near Lat 38°S: Evidence for a Genetic Relationship between continental and marine Geologic Features or a Case of Curious Coincidences?" in *In Nazca Plate: Crustal Formation and Andean Convergence*. Editors L. D. Kulm, J. Dymond, E. J. Dasch, and D. M. Hussong (The Geological Society of America), 755–760. doi:10.1130/mem154-p755

Hickey -Vargas, R., Roa, H. M., Escobar, L. L., and Frey, F. A. (1989). Geochemical Variations in Andean Basaltic and Silicic Lavas from the Villarrica-Lanin Volcanic Chain (39.5 S): an Evaluation of Source Heterogeneity, Fractional Crystallization and Crustal Assimilation. *Contr. Mineral. Petrol.* 103 (3), 361–386. doi:10.1007/bf00402922

Hickey, R., Frey, F. A., Gerlach, D. C., and López-Escobar, L. (1986). Multiple Sources for Basaltic Arc Rocks from the Southern Volcanic Zone of the Andes (34°-41°S): Trace Element and Isotopic Evidence for Contributions from Subducted Oceanic Crust, Mantle and continental Crust. *J. Geophys. Res.* 91 (6), 5963–5983. doi:10.1029/jb091ib06p05963

Hildreth, W., and Moorbath, S. (1988). Crustal Contributions to Arc Magmatism in the Andes of Central Chile. *Contr. Mineral. Petrol.* 98 (4), 455–489. doi:10.1007/bf00372365

Hilton, D. R., Hammerschmidt, K., Teufel, S., and Friedrichsen, H. (1993). Helium Isotope Characteristics of Andean Geothermal Fluids and Lavas. *Earth Planet. Sci. Lett.* 120, 265–282. doi:10.1016/0012-821x(93)90244-4

Hirose, K., and Kawamoto, T. (1995). Hydrous Partial Melting of Lherzolite at 1 GPa: The Effect of H_2O on the Genesis of Basaltic Magmas. *Earth Planet. Sci. Lett.* 133 (3-4), 463–473. doi:10.1016/0012-821x(95)00096-u

Hirose, K. (1997). Melting Experiments on Lherzolite KLB-1 under Hydrous Conditions and Generation of High-Magnesian Andesitic Melts. *Geol* 25 (1), 42–44. doi:10.1130/0091-7613(1997)025<0042:meolku>2.3.co;2

Hirschmann, M. M., Asimow, P. D., Ghiorso, M. S., and Stolper, E. M. (1999). Calculation of Peridotite Partial Melting from Thermodynamic Models of Minerals and Melts. III. Controls on Isobaric Melt Production and the Effect of Water on Melt Production. *J. Pet.* 40 (5), 831–851. doi:10.1093/petroj/40.5.831

Hora, J. M., Singer, B. S., Wörner, G., Beard, B. L., Jicha, B. R., and Johnson, C. M. (2009). Shallow and Deep Crustal Control on Differentiation of Calc-Alkaline and Tholeiitic Magma. *Earth Planet. Sci. Lett.* 285 (1), 75–86. doi:10.1016/j.epsl.2009.05.042

Hyndman, R. D., and Peacock, S. M. (2003). Serpentinization of the Forearc Mantle. *Earth Planet. Sci. Lett.* 212 (3-4), 417–432. doi:10.1016/s0012-821x(03)00263-2

Jicha, B. R., Singer, B. S., Beard, B. L., Johnson, C. M., Moreno-Roa, H., and Naranjo, J. A. (2007). Rapid Magma Ascent and Generation of 230Th Excesses in the Lower Crust at Puyehue-Cordón Caulle, Southern Volcanic Zone, Chile. *Earth Planet. Sci. Lett.* 255, 229–242. doi:10.1016/j.epsl.2006.12.017

Jicha, B. R., Singer, B. S., Brophy, J. G., Fournelle, J. H., Johnson, C. M., Beard, B. L., et al. (2004). Variable Impact of the Subducted Slab on Aleutian Island Arc Magma Sources: Evidence from Sr, Nd, Pb, and Hf Isotopes and Trace Element Abundances. *J. Pet.* 45 (9), 1845–1875. doi:10.1093/petrology/egh036

Johnson, M. C., and Plank, T. (1999). Dehydration and Melting Experiments Constrain the Fate of Subducted Sediments. Geochemistry Geophysics Geosystems 1. 1999GC000014.

Jordan, T. E., Burns, W. M., Veiga, R., Pángaro, F., Copeland, P., Kelley, S., et al. (2001). Extension and basin Formation in the Southern Andes Caused by Increased Convergence Rate: A Mid-cenozoic Trigger for the Andes. *Tectonics* 20 (3), 308–324. doi:10.1029/1999tc001181

Kay, S. M., Burns, W. M., Copeland, P., and Mancilla, O. (2006). "Upper Cretaceous to Holocene Magmatism and Evidence for Transient Miocene Shallowing of the Andean Subduction Zone under the Northern Neuquén Basin," in Evolution of an Andean Margin: A Tectonic and Magmatic View from the Andes to the Neuquén Basin (35°-39°S Lat), Eds. S.M. Kay & V.A. Ramos. (Boulder, Colorado: The Geological Society of America), 19–60.

Kay, S. M., Godoy, E., and Kurtz, A. (2005). Episodic Arc Migration, Crustal Thickening, Subduction Erosion, and Magmatism in the South-central Andes. *Geol. Soc. America Bull.* 117, 67–88. doi:10.1130/b25431.1

Kelley, K. A., and Cottrell, E. (2009). Water and the Oxidation State of Subduction Zone Magmas. *Science* 325 (5940), 605–607. doi:10.1126/science.1174156

Leake, B., Woolley, A., Arps, C., Birch, W., Gilbert, M., Grice, J., et al. (1997). Nomenclature of Amphiboles: Report of the Subcommittee on Amphiboles of the International Mineralogical Association, Commission on New Minerals and Minerals Names. *Am. Mineral.* 82, 1019–1037.

Leeman, W. P. (1996). "Boron and Other Fluid-mobile Elements in Volcanic Arc Lavas: Implications for Subduction Processes," in *Subduction: Top to Bottom*. Editors G. E. Bebout, D. W. Scholl, S. H. Kirby, and J. P. Platt (Washington DC: American Geophysical Union), 269–276.

Longhi, J. (1991). Comparative Liquidus Equilibria of Hyperstene-Normative Basalts at Low Pressure. *Am. Mineral.* 76, 785–800.

López-Escobar, L., Cembrano, J., and Moreno, H. (1995a). Geochemistry and Tectonics of the Chilean Southern Andes Basaltic Quaternary Volcanism (37-46°S). *Revista Geológica de Chile* 22 (2), 219–234.

López-Escobar, L., Kilian, R., Kempton, P. D., and Tagiri, M. (1993). Petrography and Geochemistry of Quaternary Rocks from the Southern Volcanic Zone of the Andes between 41°30' and 46°00'S, Chile. *Revista Geológica de Chile* 20 (1), 35–55.

López-Escobar, L., Moreno, H., Tagiri, M., Notsu, K., and Onuma, N. (1985). Geochemistry and Petrology of Lavas from San Jose Volcano, Southern Andes (33.DEG.45'S). *Geochem. J.* 19, 209–222. doi:10.2343/geochemj.19.209

López-Escobar, L., Parada, M. A., Hickey-Vargas, R., Frey, F. A., Kempton, P. D., and Moreno, H. (1995b). Calbuco Volcano and Minor Eruptive Centers Distributed along the Liquiñe-Ofqui Fault Zone, Chile (41°-42° S): Contrasting Origin of Andesitic and Basaltic Magma in the Southern Volcanic Zone of the Andes. *Contrib. Mineralogy Pet.* 119 (4), 345–361.

López-Escobar, L., Parada, M. A., Moreno, H., Frey, F., and Hickey-Vargas, R. (1992). A Contribution to the Petrogenesis of Osorno and Calbuco Volcanoes, Southern Andes (41°00'-41°30'S): Comparative Study. *Revista Geológica de Chile* 19 (2), 211–226.

Loucks, R. R. (2021). Deep Entrapment of Buoyant Magmas by Orogenic Tectonic Stress: Its Role in Producing continental Crust, Adakites, and Porphyry Copper Deposits. *Earth-Science Rev.* 220, 103744. doi:10.1016/j.earscirev.2021.103744

Manea, M., and Manea, V. C. (2008). On the Origin of El Chichón Volcano and Subduction of Tehuantepec Ridge: A Geodynamical Perspective. *J. Volcanology Geothermal Res.* 175 (4), 459–471. doi:10.1016/j.jvolgeores.2008.02.028

Manea, V. C., Leeman, W. P., Gerya, T., Manea, M., and Zhu, G. (2014). Subduction of Fracture Zones Controls Mantle Melting and Geochemical Signature above Slabs. *Nat. Commun.* 5 (1), 5095. doi:10.1038/ncomms6095

McManus, J. (2006). "Data Report: Major and Trace Element Data from Leg 202 Sites 1233 and 1234," in *Proceedings of the Ocean Drilling Program, Scientific Results*. Editors R. Tiedemann, A. C. Mix, C. Richter, and W. F. Ruddiman (College Station, TX: Ocean Drilling Program), 1–9.

McMillan, N. J., Harmon, R. S., Moorbath, S., López-Escobar, L., and Strong, D. F. (1989). Crustal Sources Involved in continental Arc Magmatism: A Case Study of Volcan Mocho-Choshuenco, Southern Chile. *Geol* 17, 1152–1156. doi:10.1130/0091-7613(1989)017<1152:csiica>2.3.co;2

Mella, M., Muñoz, J., Vergara, M., Klohn, E., Farmer, L., and Stern, C. (2005). Petrogenesis of the Pleistocene Tronador Volcanic Group, Andean Southern Volcanic Zone. *Revista Geológica de Chile* 32 (1), 131–154. doi:10.4067/s0716-02082005000100008

Moore, G., and Carmichael, I. S. E. (1998). The Hydrous Phase Equilibria (To 3 Kbar) of an Andesite and Basaltic Andesite from Western Mexico: Constraints on Water Content and Conditions of Phenocryst Growth. *Contrib. Mineralogy Pet.* 130 (3-4), 304–319. doi:10.1007/s004100050367

Moscoso, E., and Contreras-Reyes, E. (2012). Outer Rise Seismicity Related to the Maule, Chile 2010 Megathrust Earthquake and Hydration of the Incoming Oceanic Lithosphere. *Andean Geology.* 39 (3), 564–572. doi:10.5027/andgeoV39n3-a12

Mungall, J. E. (2002). Roasting the Mantle: Slab Melting and the Genesis of Major Au and Au-Rich Cu Deposits. *Geol* 30 (10), 915–918. doi:10.1130/0091-7613(2002)030<0915:rtmsma>2.0.co;2

Muñoz, J., and Niemeyer, C. (1984). *Hoja Laguna del Maule, Regiones del Maule y del Bío Bío. 1:250.000*. Santiago: Chile. Servicio Nacional de Geología y Minería (SERNAGEOMIN).

Müntener, O., Kelemen, P. B., and Grove, T. L. (2001). The Role of H2O during Crystallization of Primitive Arc Magmas under Uppermost Mantle Conditions and Genesis of Igneous Pyroxenites: an Experimental Study. *Contrib. Mineral. Petrol.* 141 (6), 643–658. doi:10.1007/s004100100266

Peacock, S. M. (2001). Are the Lower Planes of Double Seismic Zones Caused by Serpentine Dehydration in Subducting Oceanic Mantle? *Geol* 29 (4), 299–302. doi:10.1130/0091-7613(2001)029<0299:atlpod>2.0.co;2

Pichavant, M., Martel, C. J., and Scaillet, B. (2002). Physical Conditions, Structure and Dynamics of a Zoned Magma Chamber: Mount Pelée (Martinique, Lesser Antilles Arc). Journal of Geophysical Research 107(B5). *ECV 2-1-ECV*, 2–30.

Plank, T. (2005). Constraints from Thorium/Lanthanum on Sediment Recycling at Subduction Zones and the Evolution of the Continents. *J. Pet.* 46 (5), 921–944. doi:10.1093/petrology/egi005

Ranero, C. R., Phipps Morgan, J., McIntosh, K., and Reichert, C. (2003). Bending-related Faulting and Mantle Serpentinization at the Middle America Trench. *Nature* 425, 367–373. doi:10.1038/nature01961

Ranero, C. R., and Sallarès, V. (2004). Sallarès, VGeophysical Evidence for Hydration of the Crust and Mantle of the Nazca Plate during Bending at the north Chile Trench. *Geol* 32 (7), 549–552. doi:10.1130/g20379.1

Richards, J. P. (2015). The Oxidation State, and Sulfur and Cu Contents of Arc Magmas: Implications for Metallogeny. *Lithos* 233, 27–45. doi:10.1016/j.lithos.2014.12.011

Rodríguez, A. C. (2006). Intra-crustal Origin of Holocene Adakitic Magmas at Nevado de Longaví Volcano (Chilean Andes, 36.2°S). *Univ. Geneva*. Ph.D. ThesisAvailable at: https://archive-ouverte.unige.ch/unige:98070.

Rodríguez, C., Sellés, D., Dungan, M., Langmuir, C., and Leeman, W. (2007). Adakitic Dacites Formed by Intracrustal Crystal Fractionation of Water-rich Parent Magmas at Nevado de Longaví Volcano (36·2°S; Andean Southern Volcanic Zone, Central Chile). *J. Pet.* 48 (11), 2033–2061. doi:10.1093/petrology/egm049

Rudnick, R. L., and Gao, S. (2003). "Composition of the continental Crust," in *The Crust*. Editor R. L. Rudnick (Pergamon, Oxford: Elsevier), 1–64. doi:10.1016/b0-08-043751-6/03016-4:

Rüpke, L. H., Morgan, J. P., Hort, M., and Connolly, J. A. D. (2002). Are the Regional Variations in Central American Arc Lavas Due to Differing Basaltic versus Peridotitic Slab Sources of Fluids? *Geol* 30 (11), 1035–1038. doi:10.1130/0091-7613(2002)030<1035:atrvic>2.0.co;2

Sellés, D. (2006). Stratigraphy, petrology, and geochemistry of Nevado de Longaví volcano, Chilean Andes (36.2°S), Ph.D. Ph.D. *Univ. Geneva*. Available at: https://archive-ouverte.unige.ch/unige:436.

Sellés, D., Rodríguez, A. C., Dungan, M., Naranjo, J., and Gardeweg, M. (2004). Geochemistry of Nevado de Longaví volcano (36.2°S): A compositional atypical arc volcano in the Southern Volcanic Zone of the Andes. *Revista Geológica de Chile* 31 (2), 293–315. doi:10.4067/s0716-02082004000200008

Singer, B. S., Jicha, B. R., Leeman, W. P., Rogers, N. W., Thirlwall, M. F., Ryan, J., et al. (2007). Along-strike Trace Element and Isotopic Variation in Aleutian Island Arc basalt: Subduction Melts Sediments and Dehydrates Serpentine. *Journal of Geophysical Research* 112, B06206.

Singer, B. S., Leeman, W. P., Thirlwall, M. F., and Rogers, N. W. (1996). "Does Fracture Zone Subduction Increase Sediment Flux and Mantle Melting in Subduction Zones? Trace Element Evidence from Aleutian Arc Basalts," in *Subduction Top to Bottom*. Editors G. E. Bebout, D. W. Scholl,

S. H. Kirby, and J. P. Platt (Washington: American Geophysical Union), 285–291.

Sisson, T. W. (1994). Hornblende-melt Trace-Element Partitioning Measured by Ion Microprobe. *Chem. Geology.* 117 (1-4), 331–344. doi:10.1016/0009-2541(94)90135-x

Sisson, T. W., and Grove, T. L. (1993). Experimental Investigations of the Role of H2O in Calc-Alkaline Differentiation and Subduction Zone Magmatism. *Contr. Mineral. Petrol.* 113 (2), 143–166. doi:10.1007/bf00283225

Sruoga, P., Llambías, E. J., Fauqué, L., Schonwandt, D., and Repol, D. G. (2005). Volcanological and Geochemical Evolution of the Diamante Caldera-Maipo Volcano Complex in the Southern Andes of Argentina (34°10′S). *J. South Am. Earth Sci.* 19, 399–414. doi:10.1016/j.jsames.2005.06.003

Stern, C. R. (1991). Role of Subduction Erosion in the Generation of Andean Magmas. *Geol* 19 (1), 78–81. doi:10.1130/0091-7613(1991)019<0078:roseit>2.3.co;2

Stolper, E., and Newman, S. (1994). The Role of Water in the Petrogenesis of Mariana Trough Magmas. *Earth Planet. Sci. Lett.* 121, 293–325. doi:10.1016/0012-821x(94)90074-4

Sun, W., Huang, R.-f., Li, H., Hu, Y.-b., Zhang, C.-c., Sun, S.-j., et al. (2015). Porphyry Deposits and Oxidized Magmas. *Ore Geology. Rev.* 65, 97–131. doi:10.1016/j.oregeorev.2014.09.004

Tagiri, M., Moreno, H., López-Escobar, L., and Notsu, K. (1993). Two Magma Types of the High-Alumina basalt Series of Osorno Volcano, Southern Andes(41.DEG.06'S)-plagioclase Dilution Effect. *J. Min. Petr. Econ. Geol.* 88 (7), 359–371. doi:10.2465/ganko.88.359

Tasárová, Z. A. (2007). Towards Understanding the Lithospheric Structure of the Southern Chilean Subduction Zone (36oS-42oS) and its Role in the Gravity Field. *Geophys. J. Int.* 170, 995–1014.

Tassara, A., Götze, H.-J., Schmidth, S., and Hackney, R. (2006). Three-dimensional Density Model of the Nazca Plate and the Andean continental Margin. *J. Geophys. Res.* 11 (B09494), 1–26. doi:10.1029/2005jb003976

Tassara, A., and Yañez, G. (2003). Relación entre el espesor elástico de la litosfera y la segmentación tectónica del margen andino (15-47°S). *Revista Geológica de Chile* 30 (2), 159–186. doi:10.4067/s0716-02082003000200002

Tebbens, S. F., Cande, S. C., Kovacs, L., Parra, J. C., LaBrecque, J. L., and Vergara, H. (1997). The Chile Ridge: a Tectonic Framework. *J. Geophys. Res.* 102 (B6), 12035–12059. doi:10.1029/96jb02581

Tebbens, S. F., and Cande, S. C. (1997). Southeast Pacific Tectonic Evolution from Early Oligocene to Present. *J. Geophys. Res.* 102 (B6), 12061–12084. doi:10.1029/96jb02582

Tenthorey, E., and Hermann, J. (2004). Composition of Fluids during Serpentinite Breakdown in Subduction Zones: Evidence for Limited boron Mobility. *Geol* 32 (10), 865–868. doi:10.1130/g20610.1

Tormey, D. R., Frey, F. A., and López-Escobar, L. (1995). Geochemistry of the Active Azufre--Planchon--Peteroa Volcanic Complex, Chile (35 15'S): Evidence for Multiple Sources and Processes in a Cordilleran Arc Magmatic System. *J. Pet.* 36 (2), 265–298. doi:10.1093/petrology/36.2.265

Tormey, D. R., Hickey-Vargas, R., Frey, F. A., and López-Escobar, L. (1991). "Recent lavas from the Andean volcanic front (33 to 42°S)," in *Interpretations of Along-Arc Compositional Variations*. Editors R. S. Harmon and C. W. Rapela, 57–78. doi:10.1130/spe265-p57

Turner, S. J., Langmuir, C. H., Dungan, M. A., and Escrig, S. (2017). The importance of mantle wedge heterogeneity to subduction zone magmatism and the origin of EM1. *Earth Planet. Sci. Lett.* 472, 216–228. doi:10.1016/j.epsl.2017.04.051

Turner, S. J., Langmuir, C. H., Katz, R. F., Dungan, M. A., and Escrig, S. (2016). Parental arc magma compositions dominantly controlled by mantle-wedge thermal structure. *Nat. Geosci* 9 (10), 772–776. doi:10.1038/ngeo2788

Ulmer, P. (2001). Partial melting in the mantle wedge - the role of H_2O in the genesis of mantle-derived 'arc-related' magmas. *Phys. Earth Planet. Interiors* 127 (1-4), 215–232. doi:10.1016/s0031-9201(01)00229-1

Ulmer, P., and Müntener, O. (2005). "Adakites" formed by garnet fractionation at the base of the crust - an alternative scenario supported by field and experimental data. *Geophys. Res. Abstr.* 7 (09837).

Vergara, M., Morata, D., Hickey -Vargas, R., López-Escobar, L., and Beccar, I. (1999). Cenozoic tholeiitic volcanism in the Colbún area, Linares Precordillera, central Chile (35°35'-36°S). *Revista Geológica de Chile* 26 (1), 23–41. doi:10.4067/s0716-02081999000100002

Watt, S. F. L., Pyle, D. M., and Mather, T. A. (2011). Geology, petrology and geochemistry of the dome complex of Huequi volcano, southern Chile. *andgeo* 38 (2), 335–348. doi:10.5027/andgeov38n2-a05

Whalen, J. B., Percival, J. A., McNicoll, V. J., and Longstaffe, F. J. (2003). Intra-oceanic production of continental crust in a Th-depleted ca. 3.0Ga arc complex, western Superior Province, Canada. *Contrib. Mineralogy Pet.* 146, 78–99. doi:10.1007/s00410-003-0484-8

Zhang, Y., Gazel, E., Gaetani, G. A., and Klein, F. (2021). Serpentinite-derived slab fluids control the oxidation state of the subarc mantle. Science Advances 7(48), eabj2515. doi:10.1126/sciadv.abj2515

Conflict of Interest: Author DS is employed by Teck Resources Chile Ltda, and author AR is employed by CODELCO Chile.

The remaining authors declare that the research was conducted in the absence of any commercial or financial relationships that could be construed as a potential conflict of interest.

Publisher's Note: All claims expressed in this article are solely those of the authors and do not necessarily represent those of their affiliated organizations or those of the publisher, the editors, and the reviewers. Any product that may be evaluated in this article, or claim that may be made by its manufacturer, is not guaranteed or endorsed by the publisher.